

DOI: 10.1002/adma.201802724

**Article type: Review**

## **Designing Liquid-Infused Surfaces for Medical Applications: A Review**

*Caitlin Howell, Alison Grinthal, Steffi Sunny, Michael Aizenberg, and Joanna Aizenberg\**

Prof. C. Howell

Department of Chemical and Biomedical Engineering and School of Biomedical Science and Engineering, University of Maine, 5737 Jenness Hall, Orono, ME, 04469, United States

Dr. S. Sunny, Dr. A. Grinthal, Prof. J. Aizenberg

School of Engineering and Applied Sciences, Harvard University, 9 Oxford Street, Cambridge, MA, 021383, United States

E-mail: [jaiz@seas.harvard.edu](mailto:jaiz@seas.harvard.edu)

Dr. M. Aizenberg, Prof. J. Aizenberg

Wyss Institute for Biologically Inspired Engineering, 60 Oxford Street, Cambridge, MA, 02138, United States

This is the author manuscript accepted for publication and has undergone full peer review but has not been through the copyediting, typesetting, pagination and proofreading process, which may lead to differences between this version and the [Version of Record](#). Please cite this article as [doi: 10.1002/adma.201802724](https://doi.org/10.1002/adma.201802724).

This article is protected by copyright. All rights reserved.

Prof. J. Aizenberg

Kavli Institute for Bionano Science and Technology, Harvard University, 12 Oxford Street, Cambridge,  
Massachusetts 02138, United States

Keywords: devices, diagnostics, antifouling, adaptive material, surface coating

The development of new technologies is key to the continued improvement of medicine, relying on comprehensive materials design strategies that can integrate advanced therapeutic and diagnostic functions with a wide range of surface properties such as selective adhesion, dynamic responsiveness, and optical/mechanical tunability. Liquid-infused surfaces have recently come to the forefront as a unique approach to surface coatings that can resist adhesion of a wide range of contaminants for a variety of medical applications. Furthermore, these surfaces are proving highly versatile in enabling the integration of established medical surface treatments alongside the antifouling capabilities, such as drug release or biomolecule organization. In this review, the range of research being conducted on liquid-infused surfaces for medical applications is presented, from an understanding of the basics behind the interactions of physiological fluids, microbes, and mammalian cells with liquid layers to current applications of these materials in point-of-care diagnostics, medical tubing, instruments, implants and tissue engineering. Throughout this exploration, the design parameters of liquid-infused surfaces and how they can be adapted and tuned to particular applications are discussed, while identifying how the range of controllable factors offered by liquid-infused surfaces can be used to enable completely new and dynamic approaches to materials and devices for human health.

#### Table of Contents

1. Introduction .....	3
2. Design Parameters.....	7
2.1. Fundamentals.....	7
2.2. Solid substrates .....	7

This article is protected by copyright. All rights reserved.

2.3. Infusing liquids .....	11
2.4. Stability .....	12
2.5. Dynamic adaptability .....	16
3. Mechanisms of biological matter interaction with slippery surfaces.....	18
3.1. Physiological fluid interaction with slippery surfaces.....	19
3.2. Microbial interaction with slippery surfaces.....	22
3.3. Cell interaction with slippery surfaces.....	27
4. Applications.....	31
4.1. Point-of-Care Diagnostics.....	31
4.2. Surgical and Camera-Guided Instruments .....	34
4.3. Medical Tubing .....	36
4.4. Implants .....	37
4.5. Tissue Integration and Manipulation.....	40
5. Outlook .....	42

## 1. Introduction

The human body is one of the most extreme environments currently confronting materials design. Countless complex processes – multiphase fluids, enzymes, and signaling networks geared to actively colonize, transform, or break down nearly any foreign material – ubiquitously hinder the function of medical devices and introduce risks and complications. Blood, mucus, and fat stick to the lenses of camera-guided instruments such as endoscopes;<sup>[1]</sup> clotting and cell growth on cardiovascular stents obstruct blood flow;<sup>[2]</sup> bacteria form infectious biofilms on catheters and implants;<sup>[3,4]</sup> and protein accumulation and immune responses can block the functioning of medical

devices and implants and prevent release of drugs from drug delivery systems.<sup>[2,5]</sup> Finding a surface design strategy broad enough to counteract so many attachment and fouling mechanisms over so many length scales is a monumental task in itself, yet at the same time, biomedical innovation is leading in the opposite direction, focusing on materials and devices with increasingly specialized chemistries and surface structures that may have nothing to do with fouling resistance. With therapeutic and diagnostic functions of biomedical materials becoming increasingly reliant on targeting and self-regulation, designing for safety and efficacy often requires biointerfaces to both be shielded from and foster diverse processes at their surfaces, and, on top of that, optimize transparency, flexibility, thermal regulation, hardness, softness, and other physical qualities. Yet a living system, where every parameter – molecular, nano/microstructural, mechanical – is a signal, leaves little room to pursue antifouling and functional design separately.

The search for antifouling strategies has yielded insights that remarkably do point toward the possibility of a fundamental approach that, at least in principle, could achieve broad repellence without pre-empting other functions. A variety of surface topographies and chemistries have been shown to reduce fluid, protein, and bacterial adhesion, as well as clotting and immune responses, by effectively making solid interfaces “less solid” or less available. Nano- and microtopographies can substantially reduce the availability of stable anchoring points by creating a composite superhydrophobic air-solid interface,<sup>[6–9]</sup> while self-assembled monolayers and tethered polymers with hydrophilic, zwitterionic, or hydrophobic chemistries can create a solvent layer that shields the surface and/or introduce quasi-fluidity via long, flexible molecular chains.<sup>[10,11]</sup> The topographies and tethered chains can further incorporate specialized bioactive molecules, for example, on the structure tips or conjugated to the polymers.<sup>[12]</sup> But for these approaches to make an impact in

medical settings, they need to be much more robust. The air interface in superhydrophobic surfaces is metastable and can be displaced by complex fluids such as blood<sup>[5]</sup> or even by bacterial flagella;<sup>[13,14]</sup> hydration layers rely on hydrogen bonds that are easily broken under various solution conditions;<sup>[10,15]</sup> and both topographies and molecular layers can fail due to damage or defects.<sup>[12,14]</sup> Addressing each issue generally entails increasingly specific geometries, lengths, packing, or functional groups, narrowing the degrees of freedom for biomedical design and reducing the scope of fouling resistance. The path to enhancing antifouling behavior as well as merging it with developments in medicine may lie in starting from these approaches but thinking even further outside the box.

A look at how the complex human body keeps everything in order reveals one of its most striking and fundamental features – how wet its interfaces are. Surfaces and passageways everywhere – eyes, lungs, intestines, bones, joints; polymeric, mineralized, hairy, and porous – are infused and lined with liquid. The liquid surface not only combats fouling but is integral to everything else biological materials do. Tear films keep eyes clear of bacteria, debris, and stuck lids, while also creating the defect-free coating that makes them transparent. The liquid lining of lungs prevents infections, provides mechanical compliance for breathing, facilitates selective gas transport, and may act as a pressure-responsive gate between compartments.<sup>[16]</sup> Digestion is coordinated by a mucus layer that creates a smooth surface for food transport, mediates secretion and catalytic breakdown, and regulates nutrient uptake by the intestinal wall.

Inspired by fluid-lined surfaces omnipresent in the living world,<sup>[17–21]</sup> researchers have recently begun to integrate liquids into all kinds of synthetic materials, from metals and ceramics to polymer networks and gels, and to show how this simple idea can accomplish so many feats.<sup>[22–24]</sup>

With the entire interface mobile and unanchored, yet controlled through bulk liquid interactions with the substrate, fundamentally new types of surface behavior become possible. The atomically smooth liquid interface eliminates defects that lead to pinning and reduced mobility of both liquids and solids,<sup>[25]</sup> allowing even complex fluids to move or evaporate unimpeded;<sup>[22,26]</sup> the conformal liquid overlayer prevents contact with the solid, enabling droplets to “oleoplane” on the liquid with minimal dissipative force;<sup>[27]</sup> and adhesion of ice,<sup>[28,29]</sup> grease, and other substances is prevented or dramatically reduced.<sup>[22]</sup> At the same time, the liquid can actively redistribute on multiple length scales, enabling continuous self-healing and replenishment<sup>[30]</sup> as well as a whole new class of adaptive behaviors for manipulating surface topography, transparency, secretion, and other properties of the liquid interface.<sup>[31]</sup> This controlled multiscale mobility represents a unique, active interplay between a coating and a substrate, opening countless degrees of freedom for choosing material combinations, programming interfacial functions, and responsively tuning the properties of surfaces.

In this review we discuss the many exciting developments emerging as this system is brought to bear on some of the most challenging problems in medicine. A central question is how physiological fluids, microbes, and our own cells will respond to an engineered interface that is fully liquid yet integrated with a solid substrate. We discuss accumulating evidence that liquid-infused surfaces provide unprecedented protection against fouling by a wide range of substances and cell types, both in the laboratory and inside the body. But just as importantly, we also highlight illuminating cases that reveal new possibilities for selectively manipulating biological responses by tailoring the properties of the liquid interface and underlying substrate. Drawing on the many degrees of design freedom, we show how these capacities can and have been synergistically

combined with the materials properties offered by liquid-infused surfaces, to further both antifouling and functional advances across fields ranging from point-of-care diagnostics to surgery to tissue integration (**Figure 1**).

## 2. Design Parameters

### 2.1. Fundamentals

The two essential components of a liquid-infused surface – the solid underlying support and the liquid used for infiltration – work together to maintain a dynamic yet stable liquid overlayer. The solid can be flat or have nanoscale to microscale roughness, but must possess a surface chemistry matching the chemical nature of the infusing liquid. The liquid is then held in place on the solid substrate through a combination of van der Waals, and, if roughness is present, capillary forces.<sup>[25]</sup> The van der Waals and capillary forces together create an environment, in which it is more energetically favorable for the infusing liquid than for the contaminating liquid to wet the surface, resulting in a persistently infused surface presenting a protective liquid overlayer at the interface.<sup>[22]</sup> As long as these energy requirements are met, the specifics of the underlying solid composition, surface chemistry, and structure, as well as the infusing liquid type and character, can all be customized (**Figure 2**), providing a toolbox for controlling the dynamics, mechanical properties, and miscibility of the liquid surface, as well as for introducing responsive behaviors into the material.

### 2.2. Solid substrates

To date, solid substrates with widely varying materials properties, chemical compositions, surface geometries, and large-scale configurations have been used to create liquid-infused materials suited to specific research interests or applications. Original reports of omniphobic liquid surfaces utilized expanded perfluorotetraethylene (ePTFE), a material currently used in medicine for hernia

graft repair<sup>[32,33]</sup> and as barrier membranes<sup>[34]</sup>, infused with perfluoropolyether liquids.<sup>[22,35]</sup> These materials proved advantageous as liquid-infused substrates in that the ePTFE already had both the appropriate porosity and surface functional groups (fluorine atoms, in this case) to create a stable liquid overlayer. Others have used medical-grade plastics such as poly(ethylene terephthalate),<sup>[36]</sup> polycarbonate, polyvinyl chloride (PVC), polysulfone, polyethylene, polypropylene, polyimide, and polystyrene;<sup>[37]</sup> metals such as titanium,<sup>[38]</sup> aluminum,<sup>[28,39–42]</sup> and steel;<sup>[43]</sup> enamel,<sup>[44]</sup> glass,<sup>[45,46]</sup> fabric,<sup>[47,48]</sup> paper,<sup>[49]</sup> and even wood.<sup>[50]</sup>

When the intrinsic surface roughness is insufficient for creating a stable liquid overlayer, it can be generated by either adding a textured layer to the surface or removing a portion of the surface material to create appropriate topography. Additive approaches have included layer-by-layer deposition of charged polymers and particles to generate porous coatings on a variety of materials having arbitrary form factors, such as the inside of tubing.<sup>[41,51,52]</sup> Polystyrene microfiber webs<sup>[53]</sup> and the direct formation of aluminum oxy hydroxide (boehmite) nanostructures,<sup>[54–56]</sup> have been used to create roughness on medical devices of complex shapes. For flat surfaces, UV-initiated polymerization of common monomers, together with a porogenic solvent (which leads to porous structures upon removal) can be used to introduce a variety of surface textures (**Figure 3A**),<sup>[57,58]</sup> Other additive approaches involve non-solvent-induced phase separation and extraction processes,<sup>[59]</sup> osmotically driven wrinkling,<sup>[60]</sup> the electrodeposition of tungstite films,<sup>[43]</sup> and chemical vapor deposition of silicon nanowires.<sup>[61]</sup> Subtractive methods for creating surface structure have included the use of femtosecond laser ablation of steel (**Figure 3B**),<sup>[62]</sup> titanium,<sup>[38]</sup> plastic,<sup>[36]</sup> or polymer,<sup>[63]</sup> as well as acid etching on living enamel.<sup>[44]</sup> Microscale water droplets evaporated off a polyphenylene oxide surface, termed breath figure patterns, represent yet another



approach to creating large-area textured surfaces.<sup>[64]</sup> Although the majority of these current texturing methods result in random topography, examples of creating a highly ordered closed-cell structured surface based on colloidal self-assembly are also reported<sup>[65,66]</sup> (**Figure 3C**). Such an approach is particularly valuable for systematically studying the effects of topographic geometries and dimensions on phenomena such as the resistance of the liquid-infused surface to varying types of damage. In cases where introducing surface texture may not be practical, it is also possible to create liquid-infused surfaces simply through the addition of proper surface chemistry to a flat surface.<sup>[37,55,67]</sup>

As has been discussed in detail in previous publications,<sup>[22,68]</sup> an appropriate surface energy match between the solid support and the infusing liquid – and a relative mismatch between the solid and the contaminating substance – can be achieved either through intrinsic surface chemistry or by chemically functionalizing the surface. In the first case, the affinity between fluorinated/omniphobic surfaces of ePTFE and perfluorinated liquids<sup>[22]</sup> or between the hydrophobic surfaces of solid polyolefins, such as polymethylpentene,<sup>[69]</sup> and hydrophobic silicone oils are just a few of the examples that have yielded robust liquid surfaces. For the second case, the solid surface chemistry can be modified via direct deposition of the desired surface layer, for example by chemical vapor deposition of fluorinated volatile compounds,<sup>[70]</sup> or by chemical functionalization from the gas or solution phase. For example, the intrinsically present or introduced surface reactive groups (-OH or a generic -RG1) can be exposed to reagents containing the desired omniphobic polyfluorinated or hydrophobic tail and a reactive group that selectively and quickly react with the surface counterparts, allowing the surface chemistry of the solid support to be easily changed or modified. The list of possible chemical reactions that have been or can be used for such functionalizations is

very broad and includes reactions of halosilanes with surface hydroxyl groups, reactions between thiols and coinage metals (e.g., Au, Ag), any type of click chemistry when appropriate surface reactive groups are installed, linkages through phosphate or phosphonate reactive groups to metal-oxide/hydroxide surfaces, and many more. Silanization has emerged as the easiest and a highly modular functionalization method, mainly due to the commercial availability of various chlorosilanes and the overall simplicity of the procedure, and can be performed either through the gas phase for sufficiently volatile silanes or through the solution phase for less volatile ones.

The use of polymers that can be infused with liquid on a molecular level, such as polydimethylsiloxane (PDMS)<sup>[71–73]</sup> or poly(alkylmethacrylates)<sup>[42]</sup> with silicone-based oils, or fluorogel elastomers with fluorinated liquids,<sup>[74]</sup> has recently proven to be a robust method not only for stabilizing liquid at the interface but also for introducing self-replenishment capability.<sup>[75]</sup> Supramolecular polymers can simplify fabrication<sup>[76]</sup> and also enable incorporation of self-replenishing elements, such as embedded droplets that slowly migrate and transfer their contents to the surface of the material (discussed further in Section 2.5).<sup>[72,73]</sup> Recent work further showed how an evaporative lithography method could be used to control where these droplets were localized within the materials.<sup>[77]</sup> Other self-replenishing surfaces have been created by molding or embedding channel networks into liquid-infused PDMS to enable continuous or on-demand addition of liquid to the system.<sup>[71]</sup> The tunability and adaptability of liquid-infused polymer coatings make them a particularly promising target for future medical use; those interested in more in-depth information are directed to more specialized reviews on the subject.<sup>[78]</sup>

### 2.3. Infusing liquids

When choosing a liquid for medical applications, biocompatibility is among the most important, if not the primary, concern. This requirement can pose challenges when limited to water-immiscible lubricants, which are nearly always required when designing liquid-infused surfaces to repel water-based biological materials. Although still relatively few in number, several water-immiscible liquids are currently in use or have been used in clinical applications. Perfluorodecalin, a fully-fluorinated double-ring molecule, has been previously used as a US Food and Drug Administration (FDA)-approved blood substitute for post-operative patients, due to very high oxygen solubility in it.<sup>[79]</sup> Both perfluorodecalin and its three-ring analogue perfluoroperhydrophenanthrene (Vitreon), have been used as ocular tamponades.<sup>[80,81]</sup> These compounds are attractive as their fluorinated nature makes them inert and immiscible with both water- and oil-based compounds. Other air-stable non-fluorinated liquids include medical-grade silicone oils, which are also used as ocular tamponades<sup>[82]</sup> as well as for certain cosmetic reconstruction applications.<sup>[83]</sup> Silicone oils also have the advantage, due to their polymeric/oligomeric nature, of being able to have a fairly wide range of viscosities while maintaining their general chemical character, permitting modulation of the force required to move droplets along the surface.<sup>[42,69]</sup> Ionic liquids are another class of medically-relevant,<sup>[84]</sup> highly tunable fluids that have recently been used to create liquid-infused surfaces.<sup>[85,86]</sup> In addition to pharmaceutical-grade oils, some food-grade oils have also been explored for creating liquid-infused surfaces. Functionalizing porous polymer multilayers containing azlactone groups with primary amine-containing small molecules has enabled infusion with canola, coconut, and olive oils.<sup>[41]</sup> Immobilized liquid surfaces have also been created with almond oil,<sup>[51]</sup> sesame oil,<sup>[87]</sup> and oleic

acid,<sup>[40]</sup> all of which may be useful going forward for applications in medical settings involving either no patient contact or external contact only.

While many of the classes of liquids listed in this section, especially natural food-grade oils, are expected to be safe for many medical uses, important challenges remain that will need further focused efforts to facilitate their adoption for use in medicine. These will include obtaining regulatory approval for particular infusing liquids, developing methodologies of sterilizing the liquid-infused surfaces prior to use, and/or developing straightforward methods of applying the pre-sterilized liquids in a medical setting.

## 2.4. Stability

Stability is one of the most critical concerns when designing liquid layers that determines how well and for how long a surface will maintain its function. Liquid-infused surfaces of cameras, medical instruments, tubes, diagnostic devices and implants must be designed to withstand varying combinations of static environments, flows, droplets, multiphase interfaces, bubbles, and mechanical forces resulting from repeated insertion/extrusion as well as microbial probing. These exposures lead to opportunities for the liquid to be lost through displacement, stripping, evaporation, or any other combination of leaching phenomena. Each of these potential failure mechanisms can be prevented or otherwise mitigated, but doing so requires a fundamental understanding of the liquid layer's behavior as a function of the surface conditions when in use, as well as how such behavior changes based on the properties of the infusing liquid, the underlying solid, and the surrounding environment.

Liquid displacement occurs when the contaminating liquid pushes the infusing liquid away from the surface, allowing the contaminating liquid to contact the underlying solid directly. Recent

research has demonstrated the use of confocal optical interferometry, a technique that maps the liquid film's thickness profile with nanometer resolution, as an effective tool to analyze displacement of the liquid layer when sandwiched under static as well as moving droplets of a contaminating liquid.<sup>[69]</sup> The results have shown that on either flat or low-aspect-ratio microstructured substrates, the liquid layer underneath a static droplet can exist in three distinct forms. In the most stable case (denoted L1 in **Figure 4A**), a conformal liquid layer completely separates the drop from the solid; in the semi-stable state (L2 in **Figure 4B**), the drop sits on pockets of liquid but also contacts the solid; in the least stable case (L3 in **Figure 4C**), the drop displaces the liquid layer and sits completely on the solid. Which state is observed depends on the balance of interfacial tensions among the solid substrate, infusing liquid, and droplet, as well as on the van der Waals forces between the solid and infusing liquid. However, when the droplets were set in motion above a critical speed (in this particular case, 150  $\mu\text{m/s}$ ), the semi-stable L2 state changed to a stable L1 state due to hydrodynamic forces lifting the droplet on top of the infusing liquid layer. These results highlight that the properties of a liquid surface can be designed so that droplet motion enhances, rather than degrades, its integrity. This may be the case even in the presence of a complex fluid such as blood.<sup>[88]</sup>

Displacement of the liquid layer can also occur when a low-surface-energy infusing liquid spreads over a droplet of high-surface-energy contaminating liquid in what is known as a "cloaking" or "wrapping" layer (**Figure 5A**).<sup>[89–92]</sup> The loss of the infusing liquid from the surface when the droplet is shed can lead to eventual failure of the functional liquid layer. The formation of a cloaking layer and subsequent loss of the infusing liquid have been shown to occur, for example, when water flowing through a tube lined with an infused liquid layer is disrupted by air bubbles or air/water interfaces (**Figure 5B**).<sup>[55]</sup> However, not all types of infusing liquids will cloak all types of

contaminating materials. Miljkovic et al.<sup>[91]</sup> examined a range of both infusing and contaminating liquids for their abilities to create cloaking layers, identifying several infusing-contaminating liquid pairs that did not form cloaks (**Figure 5C**). Liquid loss caused by cloaking layers can also be minimized by keeping liquid-infused surfaces continuously immersed or choosing pairs that have more slowly-forming cloaking layers or form only smaller wetting ridges on the timescale of flow.

Shear failure of liquid-infused surfaces occurs when flow over the surface strips or pushes the liquid layer away. A systematic comparison of the ability of flat, nanotextured, microtextured, and hierarchical micro-nanotextured perfluoropolyether-infused fluoro-functionalized, boehmitized aluminum substrates to withstand shear failure induced by spinning in air, have shown that surfaces with a uniform nanotexture were most stable and able to withstand even the highest spin rate (10,000 rpm), still remaining repellent to water and ethanol droplets, unlike the other surface topographies tested.<sup>[54]</sup> Further work quantified the role that surface topography parameters can play in mitigating shear failure.<sup>[93]</sup> Specifically, the loss of the infusing liquid caused by shear can be prevented by having surface structures, either random or ordered, separated by distances equal to or less than a critical length ( $L_{\infty}$ ) determined by shear stress, interfacial tension, and the aspect ratio of the surface structures, among others (**Figure 6A**).  $L_{\infty}$  can be increased by deepening and narrowing the gaps between the structures but was found to be independent of viscosity, allowing the creation of solid surfaces designed to work interchangeably with infusing liquids of different viscosities, provided that the chemical match between the solid and infusing liquid remains. Although any damage done to the surface structures below the  $L_{\infty}$  threshold in general will not affect the overall stability of the infusing liquid layer, a liquid-infused surface that may be subjected to extensive damage can also further benefit from the use of a closed-cell solid structure such as a

honeycomb (**Figure 6B**), which increases the resistance of both the substrate and the liquid layer to damage from various forces such as touching and wiping.<sup>[65]</sup>

Evaporation can also be a concern when using liquid-infused surfaces in medical applications, as materials must often be stored until they are needed or left waiting while more pressing concerns are dealt with. Although relatively low molecular weight medically-relevant liquids such as perfluorodecalin and Vitreon can completely evaporate from a surface in as little as 30 min,<sup>[35]</sup> this can be mitigated by storing the samples under a buffer or other liquid solution until they are needed (**Figure 6C**). Other approaches to limiting evaporation include the selection of liquids such as high-viscosity medical-grade silicone oils<sup>[53]</sup> or ionic liquids with ultralow vapor pressure.<sup>[85,86]</sup> In many cases, an intermediate viscosity may prove sufficient, depending on the expected method of use.

Finally, depending on the degree of miscibility between the infusing liquid and the contaminating liquid, there exists the possibility of the two liquids mixing together. Even if initially chosen to be immiscible, the potential for mixing in medical applications may be increased as the proteins and other complex molecules present in many medical and biological fluids can act as surfactants. Recent publication<sup>[94]</sup> has described practical criteria for determining if an arbitrary combination of solid, infusing liquid, and contaminating fluid will fail due to phenomena such as mixing, or result in a successful contaminant-repelling system. However, the experimental validation of this model was focused on water and low-surface-tension liquids such as hexane, pentane, and octane; it would be desirable to develop a broad set of experimental data where the contaminating fluid is not a pure compound but a mixture, containing biologically-relevant components such as proteins and lipids, as well as other materials applicable to medical settings including surfactants and

polymers. Although a daunting task, this work would undoubtedly facilitate development of predictive models that would be of help in designing functional liquid-infused surfaces for medical applications. Additionally, where some degree of liquid mixing is unavoidable, it may be possible to create liquid-infused surfaces that are stabilized by the motion of the contaminating material on the surface.<sup>[95]</sup>

Since all the desirable functions of liquid-infused surfaces rely on stability of the liquid overlayer on top of the porous or textured substrate, finding new and more efficient ways to stabilize and modulate this overlayer is and will remain one of the central foci of both the fundamental and translational work in this field. Despite considerable achievements in this area, ensuring that the liquid-infused interface remains either stable or replenishable within the limits required for a medical application over the defined timeframe will continue to be central to the development of this technology.

## 2.5. Dynamic adaptability

The dynamic nature of the liquid and the variety of design elements for controlling its mobility can further be used to introduce new kinds of adaptive surface behaviors where – along with the molecular scale dynamics of the stabilized liquid surface – the liquid layer reconfigures on the micro- to macroscale in response to stimuli.<sup>[31]</sup> For example, if the liquid is infused in an elastic porous solid, deformations of the substrate can change the pore dimensions and create a driving force for the liquid surface to cave inward, transforming it from flat to a range of tunable microtopographies.<sup>[96]</sup> The inward driving force is countered by surface tension driving the liquid-liquid interface to remain flat, allowing the surface to produce differential topographies and optical transparencies when exposed to forces such as bending and poking (**Figure 7A**). This concept was



also applied to a surface with structural color, creating a self-reporting switchable surface (**Figure 7B**).<sup>[97]</sup> These responsive dynamics of the liquid layer can be used to design multifunctional adaptive materials that demonstrate both graded wetting behavior – with distinct speeds and stopping thresholds for different droplet chemistries – as well as tunable optical properties that can be varied from transparent to opaque. Tailoring the chemical and physical parameters of the solid and infusing liquid provide control over how global, macroscale forces will be translated into spatial patterning for different deformation modes.

Later work took this concept of liquid reconfiguration even further, creating a system in which liquid deformation inside a pore can selectively and reversibly form a channel in response to pressure from a liquid or gas (**Figure 7C**).<sup>[98,99]</sup> The chemical matching between the solid membrane and infusing liquid results in the retention of a thin layer lining the pore walls, enabling liquids or gases to flow through while reducing the ability of foulants to block the membrane and even permitting pore self-cleaning upon release of the flow-inducing pressure.<sup>[100]</sup> Theoretical modeling of the balance of forces governing pore opening and closing provides an initial framework for how the material parameters can be tailored for a wide range of liquid and gas selectivities. Dynamically adaptable surfaces have also been created by selecting an infusing liquid with switchable properties, such as temperature-activated infused surfaces that become slippery and transparent when heated, and opaque and sticky when cooled.<sup>[101–103]</sup> The effectiveness and versatility of liquid-infused surfaces in which the liquids contain bioactive small molecules, such as bacterial quorum-sensing compounds<sup>[104,105]</sup> and nitric oxide,<sup>[106]</sup> have also been demonstrated.

The use of infused polymers adds yet another level of adaptability to liquid-infused surfaces. In particular, supramolecular polymers have been used to create inducible secretion systems in which

embedded shell-less droplets of the infusing liquid responsively transfer their contents to the surface as the liquid overlayer becomes depleted.<sup>[72,75]</sup> Disjoining pressure at the gel's surface creates a driving force to restore the liquid layer to a set thickness, with the transfer of liquid from a droplet to the surface rate-limited by the rate of polymer bond reorganization at the gel-droplet interface as the droplet shrinks. Tailoring parameters such as polymer bond energy, crosslinking density, and the liquid's chemical and physical properties allows fine control over dynamic functions such as self-replenishing of the slippery surface, continuously regulated secretion of biomedically relevant liquids tied to consumption, and self-healing of the solid material. Further refinement of this strategy has yielded a method to selectively localize and pattern these droplets and enable control of the direction of droplet movement.<sup>[107]</sup> Others have used a droplet-entrainment effect to create materials that release their droplets from the polymer matrix upon exposure to sub-freezing temperatures,<sup>[73]</sup> or the incorporation of an internal vascular system to provide excess liquid for continual surface replenishment.<sup>[71,75]</sup> The ability to change the elastic modulus of infused polymers, as well as the effective pore size for controlling the movement of the infusing liquid within them, may be used to create customized dynamic properties in multiple medical applications.

### 3. Mechanisms of biological matter interaction with slippery surfaces

Although the bulk of recent research into liquid-infused surfaces has been focused on the general physics<sup>[26]</sup> and application of the concept<sup>[22]</sup> as well as resistance to low-surface-tension liquids,<sup>[91]</sup> ice,<sup>[28,29,108]</sup> and industrial foulants,<sup>[109,110]</sup> the use of these surfaces in biology and medicine has been gaining in recognition and interest.<sup>[68,111]</sup> An underlying component of this work is the additional degrees of complexity that biological systems introduce into surface interactions, and how they must be taken into account when considering design principles for the creation of materials for

eventual technology translation. Complexity in biointerfacial interactions spans multiple length and time scales and arises from the natural heterogeneity of biological material; from the addition of inter-communicating cells to that heterogeneity, such as microorganisms with the ability to mechanically probe or deform a liquid layer; and finally from the ability of communicating mammalian cells to perform advanced functions such as differentiation or the formation of tissue.

### 3.1. Physiological fluid interaction with slippery surfaces

Nearly every fluid in the body is a complex fluid – from mucus, saliva, sweat, urine, and blood to bile and fat deposits. Each has a distinct composition and viscosity, can contain complex and reactive biomolecules, and can also have active processes such as clotting taking place within the liquid phase. Moreover, tubes, instruments, and other devices that contact physiological fluids are often exposed to complex flow patterns, such as intermittent, bi-directional, drop-wise, or slug flow. Together, these conditions make fouling of materials by physiological fluids notoriously difficult to prevent.

Surprisingly, only a handful of studies have examined the interaction of physiological fluids and their components with liquid-infused surfaces. Studies of adhesion of streptavidin<sup>[52]</sup> and fibrinogen<sup>[37,106]</sup> (**Figure 8A**) to materials with liquid layers, in comparison to appropriate solid controls, have reported that following immersion little to no protein remained on the surfaces that present an immobilized liquid interface. Similar results have also been reported for mucins,<sup>[44,46]</sup> as well as artificial saliva, artificial urine, 5% bovine serum albumin solutions, and DNA solutions.<sup>[49]</sup> Whole blood droplets are reported to be completely shed at very low tilt angles and with high speeds, leaving no trail or stain behind (**Figure 8B**).<sup>[37,43,87]</sup> Interestingly, this performance is observed with a wide variety of liquid-infused materials despite substantial differences in blood droplet

contact angles on the different surfaces, ranging from  $\sim 30^\circ$  for almond oil on cross-linked chitosan films<sup>[51]</sup> to  $\sim 150^\circ$  for perfluorinated liquids on fluorinated paper.<sup>[49]</sup> Further investigations have shown that the easy shedding of blood droplets translates into longer time to coagulation and clot formation both *in vitro*<sup>[37,51,53]</sup> and *in vivo*,<sup>[37]</sup> as well as effectiveness against blood staining in a surgical setting.<sup>[46,87]</sup> This could prove highly useful when designing specialized bandages that permit healing while preventing sticking of the bandage material in the wound,<sup>[111,112]</sup> and could be combined with concepts such as Janus fabrics<sup>[113]</sup> to create multi-functional dressings for wounds where adhesion can cause significant problems, such as burns. Work demonstrating the ability of almond oil-infused surfaces to repel water at pH levels from  $\sim 2$  to  $\sim 11$  (**Figure 8C**) suggests that this approach holds promise to be effective at repelling a wide range of body fluids as well.<sup>[51]</sup>

While the clearest applications of liquid-infused surfaces for contact with physiological fluids capitalize on their anti-adhesion properties, resisting staining, fouling, and clotting, there have also been reports of using liquid layers to control the behavior of biological molecules in more diverse ways. One recently published example<sup>[114]</sup> describes a new tissue engineering strategy involving a way to create a stable fibronectin layer on a silicone oil-infused polymer surface: by removing the majority of the liquid layer from the surface before immediately depositing the protein on top. The fibronectin formed a network on the residual liquid at the surface, remaining suspended on top of the liquid layer as it self-replenished from the bulk of the infused polymer. This layer was then used to grow a sheet of stem cells that could be easily released from the surface. In another interesting design, the liquid surface has enabled unique manipulation of biomolecules inside droplets.<sup>[115]</sup> Upon placing two water droplets containing amphiphilic phospholipids on an infused surface and allowing them to touch, a stable lipid bilayer formed and replaced the cloaking layer at the droplet-droplet

interface. Incorporating transmembrane peptides enabled formation of ion channels across the bilayer, allowing electrical characterization of channel properties under ambient conditions for the first time.

For the most part, detailed molecular studies of how exactly the proteins and other biological molecules in physiological fluids interact with the infused liquid layer, and how this differs from or is similar to bulk or emulsion interfaces, remain to be done. The spontaneous adsorption of proteins at bulk or droplet-immiscible liquid interfaces has been studied more in-depth in the context of the food and cosmetics industries,<sup>[116]</sup> where proteins are used as surfactants to decrease the amount of energy necessary to form emulsions and increase overall emulsion stability.<sup>[117]</sup> When adsorption occurs under these conditions, the native structures of the proteins partially unfold, leading to the exposure of hydrophobic or sulfhydryl residues that are otherwise hidden in the aqueous phase. Such a transition can lead to the creation of interfacial networks over the interface, which can be made stronger by using proteins with more rigid initial internal structural bonding.<sup>[116,118]</sup> On a functional level, trapping of some types of enzymes, such as lipases, at a bulk or droplet liquid-liquid interface can also either activate or enhance their catalytic activity.<sup>[119,120]</sup>

Building on this concept, liquid-infused surfaces could be used as a way to control the interactions of proteins and other biomolecules at liquid-liquid interfaces for biochemical reactions or molecular synthesis<sup>[121]</sup> that is easier to handle than bulk liquid-liquid interfaces. How biomolecular phenomena will differ on an infused liquid layer compared to a bulk interface will need to be investigated, and will likely differ from infusing liquid to infusing liquid, and perhaps also among different textures and composition of the underlying solid.

### 3.2. Microbial interaction with slippery surfaces

While designing materials to resist the adhesion of blood and other physiological fluids presents a grand challenge in and of itself, developing materials to resist adhesion by living systems such as bacteria and other microorganisms requires considering an entirely new level of complexity. Bacteria are tremendously successful at adhering to and colonizing surfaces due to their ability to adapt and change. Significant evidence exists of the ability of these microorganisms to sense surfaces,<sup>[122–124]</sup> respond to them by either physically perturbing their environment<sup>[14]</sup> or altering gene expression to induce biofilm formation,<sup>[125]</sup> communicate with surrounding bacteria to initiate coordinated activity,<sup>[126,127]</sup> and over time physically evolve to be better suited to thrive, even in the face of challenging environmental conditions<sup>[128,129]</sup> or the application of antibiotics.<sup>[130]</sup> Methods to combat bacterial surface adhesion such as surface modification through plasma treatment,<sup>[131]</sup> surface grafting of antifouling polymers such as poly(ethylene)glycol,<sup>[132]</sup> the immobilization of antimicrobial peptides and biofilm-dispersing enzymes,<sup>[4]</sup> or the use of superhydrophobic or bio-inspired textured surfaces,<sup>[133]</sup> while frequently successful in the short-term or in monoculture conditions, can nearly always be overcome in time by a complex, dynamic, living bacterial system. This fact is especially concerning in medicine, where bacterial colonization of surfaces frequently leads to the use of antibiotics and a higher likelihood of the development of drug-resistant strains.<sup>[134,135]</sup> To combat this, the development of more tools to enhance our current technologies or provide alternatives are needed.

Several different types of liquid-infused surfaces have been tested against a variety of bacterial species, validating the initial concept that this approach can be an effective new tool to combat bacterial adhesion. Early work using liquid-infused surfaces fabricated by immobilizing

perfluoropolyether liquids on ePTFE showed that these materials could reduce biofilm coverage of *Escherichia coli* by 96.0% and *Staphylococcus aureus* by 97.2% after 48 h, as well as *Pseudomonas aeruginosa* by 99.6% after 7 days of growth at low flow rates (10 ml/min).<sup>[136]</sup> Recent applications of this concept *in vivo* have demonstrated that this principle continues to hold true in living systems, reducing bacterial load in an infected hernia implant model<sup>[35]</sup> and inhibiting biofilm formation in a dental plaque model.<sup>[44]</sup> Researchers working on the ability of liquid-infused surfaces fabricated using solid-liquid combinations other than ePTFE-perfluoropolyether fluid to resist bacterial and biofilm adhesion have also found promising initial results. Solids textured by LbL deposition,<sup>[104,105]</sup> UV-initiated polymerization,<sup>[58]</sup> or osmotically-driven wrinkling<sup>[60]</sup> and coated with either perfluorinated or silicone liquids have also proven generally effective at resisting both bacterial and fungal biofilm adhesion, frequently preventing more than 97% of the biofilms from remaining on the surfaces (**Figure 9A,B**). Multiple reports have also demonstrated the ability of silicone oil-infused PDMS and other silicone compounds, separately already widely used in medicine, to resist *S. aureus*, *P. aeruginosa*, and *E. coli* biofilm attachment under both static<sup>[37,58,71,137]</sup> and flow conditions (**Figure 9C**).<sup>[37,137,138]</sup>

Beyond simple adhesion or non-adhesion, liquid surfaces have also produced some surprising and illuminating results in the cases where microbes do attach to them. For example, while dense bacterial attachment almost invariably leads to biofilm formation on synthetic solid surfaces, this may not be the case on a liquid surface. In a recent study, silicone oil-infused PDMS showed a significant number of *E. coli* colony-forming units, comparable to non-infused PDMS, under orbital flow, despite preventing all attachment under static conditions.<sup>[137]</sup> Yet surprisingly, the infused PDMS samples still showed minimal biofilm coverage under both flow and static conditions,

suggesting the progression to biofilm formation may have been blocked. Furthermore, while liquid-infused surfaces appear to disrupt a very wide diversity of biofilm formation mechanisms, a multidrug-resistant strain of *P. aeruginosa* isolated from wastewater displayed up to 12% biofilm coverage on perfluorinated liquid-coated surfaces, while its antibiotic-susceptible counterparts averaged less than 1% coverage.<sup>[58]</sup> In another anomalous result, *E. coli* that had been sprayed via microdroplets designed to simulate a sneeze or cough – rather than in bulk medium – were unexpectedly more difficult to remove from a silicone oil-infused PDMS surface than from a traditional textured superhydrophobic surface.<sup>[139]</sup> The authors hypothesized that a cloaking layer may have formed over the smaller bacteria-containing droplets (see Section 2.4) on the liquid surface and prevented them from sliding away. With greater understanding of these interactions, liquid surfaces may offer not only basic insight into how surface mobility influences microbial colonization, but opportunities to design future materials that take advantage of controlled liquid interactions to provide new and responsive properties such as selective, reversible trapping of pathogenic microorganisms, or the capture of bacterial cells in a manner that does not allow them to form a biofilm or that controls inter-cell communication via wrapping layer interfaces. However, the first step toward realizing this goal is a better understanding of the fundamentals behind how bacteria interact with immobilized liquids.

Bacterial surface responses are mediated in part by their cellular structures, including flagella, fimbriae, and pili, through which they mechanically sense their surroundings.<sup>[123]</sup> Of these, the interruption of the rotational motion of flagella, for example by a solid surface, has been shown to play a large role in the initiation of biofilm growth in a number of species including *E. coli*,<sup>[140]</sup> and *Vibrio cholera*,<sup>[141]</sup> or induce the formation of swarmer cells in other species such as *Vibrio*



*parahaemolyticus*<sup>[142]</sup> and *Proteus mirabilis*.<sup>[143]</sup> The effect of viscosity on this response has been identified for *P. mirabilis* using increasing concentrations of agar to create increasingly viscous surface conditions.<sup>[144]</sup> The use of liquid-infused surfaces could enable further such investigations with liquids of varying properties to more closely simulate physiological interface conditions, while answering fundamental questions about how bacteria interact with and respond to dynamic surfaces, including how a liquid of variable viscosity may affect the activation of biofilm initiator genes<sup>[145]</sup> by presenting something other than a solid surface. This knowledge in turn should permit the design of increasingly more effective liquid-solid combinations.

The interactions of bacteria with immiscible liquid-liquid interfaces have been studied in other contexts, particularly in food safety<sup>[146]</sup> and oil bioremediation.<sup>[147]</sup> Initial attachment is influenced by the complex hydrophobic and hydrophilic surfaces of both the cell body and appendages, as well as environmental conditions including pH, medium composition, growth stage, and cell mobility.<sup>[146,148]</sup> Bacteria are also known to produce a range of different types of surfactants<sup>[149]</sup> that can facilitate and enhance bacterial adhesion to hydrocarbon and other hydrophobic interfaces.<sup>[150]</sup> Together, this makes for a complex set of interactions that lead to variable outcomes. It is known that bacteria can form biofilms at oil/water interfaces,<sup>[151,152]</sup> although the structure and adhesive strength of such biofilms can vary significantly among species.<sup>[151]</sup> Preliminary work using immobilized liquid layers has also revealed evidence of biofilm formation at their oil/water interfaces<sup>[153]</sup> that can differ between species<sup>[137]</sup> and strains.<sup>[58]</sup> The first reports of microorganism growth on layers of silicone oil on PDMS noted a “peeling away” of a combined bacterial/algal biofilm that had formed on the oil layer when the samples were exposed to an air/water interface, often leaving an intact biofilm floating on the surface of the liquid medium<sup>[71]</sup>

(Figure 10A). This process may prove useful as a technique to study biofilm structure and composition, allowing direct access to the interface-contacting side of the biofilm. When the surface is patterned with an infusing liquid creating adhesion-promoting areas surrounded by liquid-infused borders, removal of the biofilm can result in arbitrarily-shaped and discrete biofilms (Figure 10B).<sup>[154]</sup>

As living organisms that can adapt, bacteria are exceptionally good at overcoming obstacles to attachment. This fact makes it unlikely that any single surface modification approach will work to resist colonization in the long term, even one with the dynamic nature of liquid. However, liquid-infused surfaces can also be used as a vehicle to synergistically bring together multiple antibacterial and anti-adhesion strategies in ways that cannot be easily accomplished with solid surfaces. For example, liquid infused in LbL surfaces could be used to sustain the release of the antimicrobial compound triclosan.<sup>[104]</sup> This approach allowed for not only the prevention of surface adhesion by the yeast *Candida albicans*, but also the near elimination of metabolically-active *C. albicans* in the surrounding solutions. Further work by the same group<sup>[105]</sup> demonstrated this concept also worked with small-molecule quorum-sensing inhibitors, preventing the growth of *P. aeruginosa* both directly on a sample and on the surface surrounding the sample (Figure 11A).

A similar approach to creating a functional liquid interface for enhanced bacterial resistance used a bio-inspired method to continuously replenish the surface liquid layer, embedding a vascular system filled with excess lubricating liquid into a permeable polymer sample.<sup>[71]</sup> In this case, silicone oil was used; however, this approach could be applied to a range of different polymer/liquid combinations. When the surface liquid layer was removed through evaporation, the liquid from the vascular channels diffused up through the polymer to the surface, replenishing the surface liquid layer. This approach was found to enable continuous resistance to *S. aureus* biofilm formation over

the course of 48 h of intense liquid overlayer removal (**Figure 11B**),<sup>[71]</sup> and may further prove useful in controlling the timing and spatial definition of compounds delivered to bacteria at the interface.

### 3.3. Cell interaction with slippery surfaces

Human cells combine the most complex of both worlds: like physiological fluids, a single cell can potentially interact over much larger surface areas than a bacterium, yet its responses are coordinated by a dense network of signaling cascades across the whole cell. These capacities raise basic questions concerning how or if liquid-infused surfaces can be designed to avoid invoking the cellular responses triggered by most other types of surfaces. At the same time, the body's own cells present design with a conundrum – materials should repel them to avoid triggering immune attack and fibrotic capsule formation, yet must also often be programmed to act as scaffolds for tissue development, wound healing, and other surface behaviors. The enormous signaling and structural complexity within each cell in principle offers numerous opportunities to select, dissect, and manipulate the many facets of the surface-triggered response at the single cell level, but it has rarely been explored how something as simple but fundamental as a liquid might be used to influence the progression of events in the course of cells' interaction, attachment, and growth.

*In vitro* studies of liquid-infused surfaces in contact with cells, including fibroblasts,<sup>[38,74,155]</sup> osteoblasts,<sup>[38,156]</sup> stem cells,<sup>[46]</sup> glioma cells (**Figure 12A**),<sup>[36]</sup> breast cancer cells,<sup>[155]</sup> macrophages,<sup>[35]</sup> erythrocytes,<sup>[37]</sup> and platelets,<sup>[37,60]</sup> have shown that liquid surfaces can prevent the attachment and proliferation of multiple cell types despite differences in their size, shape, surface chemistry, and signaling mechanisms. In addition to preventing undesired interactions, this capacity to control cell adhesion has been used in a variety of creative and potentially transformative ways. Micropatterns of both single<sup>[157]</sup> and multiple<sup>[155]</sup> cell types have been created by using the liquid-infused areas as

long-term, durable boundaries to prevent the cells from moving outside the defined areas (**Figure 12B**). By leveraging the fact that the surface can prevent the adhesion of both cells and other complex materials, liquid-infused surfaces were used to create shape-controlled microgel beads with encapsulated osteoblasts in a process that did not require the use of surfactants<sup>[156]</sup>. The first *in vivo* study<sup>[37]</sup> has shown that platelets in contact with a liquid-infused material not only exhibit reduced adhesion but remain round, consistent with an inactivated state (**Figure 12C**), supporting *in vivo* evidence that the surfaces are capable of reducing thrombus formation.

Recent preliminary results further suggest the intriguing possibility that a liquid surface may be able to intervene at specific stages of a cell's surface response behavior.<sup>[88]</sup> Real-time tracking of fibroblasts – cells that play a crucial role in both fibrotic capsule formation and producing secretions for wound healing – has revealed that a liquid-infused surface, silicone oil-infused PDMS, triggers secretion of potential tethers, but inhibits subsequent adhesion and downstream responses. Cells extend and retract filopodia as they probe and move over the liquid surface, as they do on a non-infused PDMS surface – but instead of attaching, they continue moving, probing, and secreting for hours, with their secretions simply floating alongside them (**Figure 13A**). The use of confocal optical interferometry<sup>[69]</sup> in these studies allowed the cells' surface responses to be spatiotemporally correlated with a detailed map of the liquid layer's thickness and integrity, and indicated that all stages of the observed behavior take place on an intact liquid surface, with no evidence of the cells penetrating or removing the liquid. However, cell behavior on areas of the infused surface that had spontaneously dewetted – and are known to retain a thin liquid oil or oil/polymer layer – hints at the additional possibility of intercepting the cell's surface repertoire at a later stage. While cells do settle on these areas, their downstream morphological response nevertheless appears to be inhibited,

resulting in diameter of 20  $\mu\text{m}$  on the minimal oil layer compared to 100  $\mu\text{m}$  on non-infused PDMS.<sup>[88]</sup> Although preliminary, these observations suggest that it would be interesting to explore whether manipulating the thickness of the liquid layer might provide a tunable way to selectively manipulate different stages of a cell's surface behavior.

Further highlighting the idea of selective cell manipulation, dynamic variation of the liquid layer has recently been used to first grow and then detach an intact cell sheet.<sup>[114]</sup> In these studies, the liquid overlayer was intentionally removed from the surface of silicone oil-infused PDMS, and fibronectin was deposited on the residual liquid interface. As discussed in Section 3.1, the fibronectin self-organized to form a contiguous surface coating, yet as the liquid overlayer was replenished with oil from the bulk PDMS, the fibronectin rose with the liquid and remained on top of it, rather than adhering to the PDMS, allowing the entire sheet to be removed with an excess bolus of oil introduced underneath it (**Figure 13B**). This time-dependent behavior on, and of, the liquid layer solves the conflict between two core requirements for cell sheet production: that cells need to be able to form strong surface attachments to grow, while still being detachable for further use. Mesenchymal stem cells start to grow following fibronectin assembly on the residual liquid interface, forming sufficient attachments to the fibronectin and each other to continue growing and integrating as the liquid layer replenishes. Once the full liquid layer is restored, an intact cell sheet with a fibronectin base layer sits on top of it and can be easily removed for further use, without loss of viability or ability to grow and proliferate.<sup>[114]</sup>

The ability of the liquid interface to prevent or intervene in cellular surface responses raises the question of whether toxicity of the infusing liquid itself may be playing a role. Although work with microorganisms has shown little to no toxicity of silicone oils<sup>[71]</sup> and perfluorinated liquids<sup>[136]</sup> at

exposure levels expected from surfaces infused with these liquids, mammalian cells can be more delicate and may therefore be more vulnerable to the presence of relatively large amounts of an immiscible liquid in their environment. To address this, the number of live and dead mouse mesenchymal stem cells grown either on or in contact with a silica LbL-coated surface infused with either a perfluoropolyether or a silicone oil was quantified.<sup>[46]</sup> In both cases, the number of dead cells was near zero, similar to a glass control. The study of Krytox perfluoropolyethers (GPL 100, 104, 105, 106, or AZ 143) mixed with a suspended cell culture to create an emulsion has shown no significant difference in cellular metabolism relative to controls for 5% (v/v) perfluoropolyether in cell medium; a significant decrease occurred only at 10% and 20% (v/v) loading of perfluoropolyether.<sup>[38]</sup> A recent *in vivo* study<sup>[35]</sup> took the question of cellular toxicity further, examining the ability of macrophages to retain their function on liquid-infused surfaces vs a solid control. When comparing number of bacteria phagocytosed over a 1 h time period, they found no significant differences between the macrophages on a liquid-infused material and a control solid surface (**Figure 14**), despite the fact that the macrophages on the infused surfaces were clearly moving with the liquid overlayer. Although toxicity must be assessed for each infusing liquid individually, these results strongly suggest that when a commonly-used medical-grade liquid is chosen, cytotoxicity is not expected to be an issue or can be further moderated by adjusting amounts and times of exposure.

## 4. Applications

### 4.1. Point-of-Care Diagnostics

Ultra-slippery and non-fouling materials not only promote longevity but, at the same time, present numerous tunable features that can be leveraged to create diagnostic systems that are able to direct and control complex biological samples with little to no sample loss in transit. For example, the ability of a liquid droplet to slide with very little external energy input has enabled a variety of novel strategies for fine control of droplet motion toward the creation of channel-free microfluidics. Multiple groups have created surfaces on which the direction of movement is pre-defined by the pattern of the liquid surface, where the liquid provides a low-friction environment that allows the droplet to slide freely, and resistance can be introduced via disruption of the liquid layer through surface chemistry<sup>[44]</sup> or the topography of the underlying solid surface.<sup>[102,158]</sup> In one approach,<sup>[142]</sup> a controlling surface topography can be revealed upon exposure to water to create a line of discrete, smooth liquid points for a droplet to move along (**Figure 15A**).

The dynamic adaptability of liquid-infused surfaces has enabled numerous systems in which the sliding of the droplet can be started and stopped on demand by altering the continuity or character of the liquid layer, for example by stretching the surface,<sup>[96]</sup> applying a voltage,<sup>[159]</sup> increasing the temperature,<sup>[101,102]</sup> or introducing a surface acoustic wave<sup>[160]</sup> to the material. Furthermore, with such systems it is possible to create differential sliding rates<sup>[145]</sup> and stop/start thresholds<sup>[96]</sup> for droplets with different surface tensions or compositions. In yet another creative use of the combination of liquid and solid properties, an imbalance in interfacial tensions along a liquid-infused shape gradient has been designed to enable spontaneous movement along a flat surface (**Figure 15B**),<sup>[161]</sup> eliminating the need to tilt samples to begin droplet movement. Pressure-responsive liquid-infused pores have also been used to guide liquid through enclosed channels.<sup>[162]</sup>

These droplet-control approaches have been tested nearly exclusively on water and other pure liquids. Therefore, the next steps for this line of research will be to demonstrate how such controlled and on-demand droplet motion can be utilized for complex physiological fluids such as blood, and how this can be used to enhance the functioning of POC diagnostics such as through the efficient delivery of physiological fluids to detection areas.

While fine control of droplet motion has received the most attention, ongoing work has also explored other ways liquid-infused surfaces can be used to enhance phenomena of potential breakthrough importance to POC diagnostic development. In one example,<sup>[49]</sup> it has been demonstrated how liquid-infused paper surfaces could be made gas-permeable but liquid-impermeable, and applied to create a colorimetric reaction in a liquid in response to the presence of a gas (**Figure 15C**). Such an approach could be used to enable low-cost, user-friendly methods for detecting the presence of certain gas-responsive chemicals in physiological fluids. In another example, liquid-infused surfaces were used to concentrate an analyte with little to no sample loss. Early on, researchers recognized that droplets undergoing evaporation on these surfaces were not subject to the coffee-ring effect, or the tendency of particles within an evaporating droplet to concentrate at the outside edge due to the pinning of the contact line.<sup>[26]</sup> This fact was then leveraged to dramatically increase the sensitivity of surface-enhanced Raman scattering to the detection of Rhodamine 6G by using evaporation to concentrate nearly all the molecules into a single point.<sup>[163]</sup> A similar approach was used to concentrate caffeine samples into multiple discrete spots on an assay strip, which could then be assessed visually.<sup>[164]</sup> Given that limits of detection can be a defining factor in many POC diagnostics, this is an important result.



Among the non-trivial developments in the application of liquid-infused surfaces toward enhanced diagnostics has been work demonstrating how initially undesirable or unexpected outcomes can be beneficial and enable new methods of detection. For example, while many applications of liquid-infused surfaces can be hindered by the presence of a cloaking layer around a droplet, as described in Section 2.4, it has been demonstrated<sup>[115]</sup> how this layer can instead be used to form a stable phospholipid bilayer between two non-coalescing droplets on a surface – a valuable technique with the potential to permit testing of the electrical character of ion channels. By inserting an electrode into each droplet on either side of the layer, the authors were able to characterize ion channel transport under ambient air conditions (**Figure 15D**).

Liquid crystal systems have also emerged as a promising new direction that is ripe for application to diagnostics, with implementation facilitated through liquid-infused surfaces. Recent work has shown how liquid crystal surfaces and shapes can be highly sensitive to low concentrations of toxins,<sup>[165]</sup> as well as how their ordering properties control and respond to bacterial mobility.<sup>[166]</sup> In addition, liquids composed of solvent-free proteins have been designed to retain gas-binding and catalytic functions.<sup>[167]</sup> Synergy between these liquids' responsive properties and the mechanical and chemical forces imposed on them by the underlying microstructure holds possibilities for generating an even greater diversity of responses, enabling the composite surfaces to be designed for finer discrimination and sensitivity. When combined with recent progress creating substrates for liquid layers in a large-scale, roll-to-roll process,<sup>[168]</sup> these approaches could prove an enabling as well as cost-effective breakthrough for diagnostics.

## 4.2. Surgical and Camera-Guided Instruments

Surgical and diagnostic instruments that enter the body must be designed to withstand the stress and strain associated with being forced through tissues ranging from skin to tendon to bone. Often, this is coupled with the need to preserve special functionality such as optical transparency of endoscope and laparoscope lenses or the articulated movement of joints in surgical robots in the face of repeated contact with multicomponent mixtures of fluids and tissues, as well as the need to minimize the unintended transmission of infectious agents such as bacteria from one area to another. Liquid-infused surfaces are currently being explored as a mechanism to permit the retention of specific materials properties such as strength or transparency, while providing an antifouling surface that can both increase the time-to-failure due to fouling and reduce cross-contamination.

The ability to fabricate liquid-infused surfaces on metals, thereby retaining strength and durability, is a critical component of the application of this technology to surgical instruments. Although work in this area is just beginning, reports of liquid-infused surfaces on titanium,<sup>[38]</sup> aluminum,<sup>[28,39–42]</sup> steel,<sup>[43]</sup> as well as iron and copper<sup>[42]</sup> are already present in the literature. In particular, a strategy has recently been introduced for electrodepositing highly durable nanoporous tungsten oxide films on various shapes of medical-grade steel, creating surfaces that resist tensile, compressive, abrasive, and impact forces due to strong chemical bonding and nanoscale morphology.<sup>[43]</sup> Following fluorination and liquid infiltration, these mechanical properties, combined with the natural self-healing and corrosion-resistance of the liquids, enable slippery surfaces to maintain their integrity in the face of numerous harsh conditions.<sup>[23]</sup> When created on steel scalpels, in addition to resisting surface staining by whole blood and transfer of *E. coli* from one place to

another (**Figure 16A**), the liquid layer decreased ripping and tearing damage when the instrument was used to cut through silicone tissue analogs,<sup>[43]</sup> presumably due to the reduced friction made possible by the slippery surface. This effect was demonstrated even more dramatically on high-temperature surfaces designed to mimic the conditions faced by electrified surgical instruments<sup>[169]</sup>. Liquid-infused surfaces led to an 80% reduction in soft tissue adhesion force at 250°C compared to non-infused controls (**Figure 16B**).

Given the move toward minimally-invasive surgeries, the inclusion of liquid-infused layers on endoscopes to increase image clarity and reduce the frequency and duration of fouling is of significant interest. Multiple reports<sup>[45,59,64,65,170]</sup> have examined the ability of an infusing liquid to further increase transparency of textured material and even enhance light transmission,<sup>[65]</sup> due to matching of the refractive index of the structured solid and the infusing liquid combined with the creation of a smooth liquid surface. The development of this concept has led to the creation of transparent liquid-infused surfaces that are flexible,<sup>[171]</sup> patternable,<sup>[65,112]</sup> able to be applied to arbitrarily-shaped surfaces,<sup>[52]</sup> and capable of having their transmission tuned by either stretching<sup>[96]</sup> or altering the material temperature.<sup>[74,101]</sup> Initial *in vivo* work examining endoscopes with camera lenses coated with a liquid-infused layer have shown clearer images compared to uncoated controls.<sup>[46,87]</sup> In a porcine bronchoscopy model, the inclusion of a liquid-infused layer on the surface of the camera lens resulted in either the ability to avoid, or ~10-15-fold shortening of, lens-cleaning processes mid-procedure (**Figure 16C**),<sup>[46]</sup> significantly decreasing the total time necessary to complete the endoscopy. Recent work has taken steps to translate this technology to the clinic by creating easily-attached, disposable cover sheets with liquid-infused layers that can be applied by clinicians on-site immediately before a procedure.<sup>[172]</sup> The use of liquid-infused coatings for

laparoscopes and endoscopes is a promising approach to improving patient outcomes and reducing complications, and may further permit the miniaturization of endoscopes by removing the need for a suction/irrigation port. Smaller optical devices would in turn permit access to narrower passages within the lungs and vasculature, increasing the areas of the body that physicians can image.

### 4.3. Medical Tubing

Tubing is ubiquitous in medical settings, and can come in the form of urinary catheters, IV lines, central venous catheters, peripherally inserted central catheter lines, spinal or intrathecal catheters, air hoses, haemodialysis catheters, and many others. The enclosed environment inside medical tubing can be particularly susceptible to fouling, with potentially life-threatening consequences to the patient. The nature and type of fouling depends on the type of material in contact with the tubing – ranging from blood, urine, or medicine to microbe-laden air – as well as the duration of contact, which can range from a few hours for intermittent-use urinary catheters<sup>[173]</sup> to over a year for some long-term central venous access devices.<sup>[174]</sup> For urinary catheters, fouling results in an infection rate of 5% per day, requiring patients to undergo re-catheterization every 3-8 days to prevent urinary tract infections.<sup>[175]</sup> In long-term central venous catheters, the formation of thrombi or the precipitation of incompatible drug mixtures can result in occlusions, leading to pulmonary and other complications as well as increasing the chance of infection.<sup>[176]</sup> For these reasons, technologies that can help to mitigate the fouling and occlusion of medical tubing and associated negative patient outcomes are of interest to the medical community.

Work on tubing in which the interior is lined with a liquid-infused layer has shown that this approach can significantly reduce bacterial biofilm formation<sup>[138]</sup> (**Figure 17A**) as well as decrease thrombus formation on both the inside and outside of catheters (**Figure 17B**).<sup>[70]</sup> In a porcine *in vivo*

model,<sup>[37]</sup> a liquid-infused layer on the inside of an arterio-venous shunt was able to permit the continuous flow of blood in the absence of systemic anticoagulants for 8 h (**Figure 17C**). Future applications of this technology could benefit from exploring the integration of the antifouling surface with other functional elements, such as drug delivery or colorimetric indicators to enable continuous monitoring of the integrity of the liquid layer. The creation of liquid layers using materials containing known therapeutic or antimicrobial components may also be an area of interest. For example, a liquid-infused substrate incorporating silver ions may function as an enhanced microbial-repellent surface<sup>[177]</sup> given that silver is known to have antimicrobial properties.<sup>[178]</sup> Furthermore, recent work<sup>[98,99]</sup> demonstrating the ability of membranes coated with liquid layers to selectively separate gases from liquids flowing through tubing may prove useful in the reduction of incidences of air embolisms, which can result from some invasive medical procedures such as cardiothoracic and neurosurgery as well as deep-water diving.<sup>[179]</sup>

#### 4.4. Implants

Medical implants are of growing importance in modern medicine, and can be found in nearly every part of the human body. A common feature of all implants, whether made from synthetic materials such as plastics and metals or natural materials like bone and transplanted tissue, is the need to withstand both the physical and biological complexities of the human body, including variable forces from surrounding tissue and fluids, immune responses, and attempts at colonization by microorganisms. This can be a particularly challenging environment for surface coatings, which are often first to encounter these environmental stresses. Although a great deal of work has been dedicated to exploring and implementing various types of materials and coatings for implants of all varieties,<sup>[180]</sup> there is a continuous need for solutions that can support tissue integration and fouling

resistance while preserving the materials strength, flexibility, or functionality required for each individual implant application.

Most investigations of liquid-infused surfaces in relation to implants have, to date, focused on *in vitro* investigations, including the resistance of various coated metals to fouling by physiological fluids, bacteria, and cells in bench-scale tests (see Sections 3.1-3.3). However, initial applications of this concept *in vivo* suggest that the promising results obtained in bench testing translates into success in living systems as well. Using a rat hernia model, it has been demonstrated *in vivo* that hernia repair meshes with infused liquid layers could prevent device infection after being exposed to a high load of *S. aureus* (**Figure 18A,B**), whereas control meshes with no liquid layer could not.<sup>[35]</sup> These results were obtained with medical-grade ePTFE, a material currently used for clinical hernia repair, as well as with liquids that are currently used in ophthalmic surgery<sup>[66,163]</sup> and have also been previously approved as blood substitutes.<sup>[65]</sup> The results showed a significant reduction in implant infection rate at 3 days post-exposure to *S. aureus*, and were attributed to the liquid layer masking the niches within the membrane material that otherwise would have provided a protective growth surface for the bacteria.<sup>[35]</sup>

Using a different approach, liquid-infused surfaces were directly created on the enamel of rabbit teeth, through a process involving acid etching and silanization with a fluorinated compound.<sup>[44]</sup> When a fluorinated liquid was placed over the treated tooth surface, staining was significantly reduced compared to an adjacent untreated control tooth in rabbits that were fed a high sucrose diet for 48 h (**Figure 18C**). The authors did note that there was some staining on the liquid-infused surface, however, suggesting that the layer formed by the liquid-solid combination chosen may not have been able to adequately withstand the forces associated with biting and

chewing. To overcome this, continued developments in creating more durable,<sup>[65,86]</sup> self-replenishing,<sup>[71,72]</sup> or additionally bioactive<sup>[104,105]</sup> materials could be leveraged.

Corrosion is also known to be a factor in the selection of materials and surface treatments for medical implants,<sup>[181,182]</sup> with metals such as aluminum, iron, magnesium and carbon steels discarded early on as options due to their reactivity within physiological fluids and tissues.<sup>[182]</sup> Investigations into how liquid-infused surfaces can be used to prevent corrosion<sup>[39,183,184]</sup> may suggest pathways to re-open possibilities for the use of these more reactive materials by masking their surface properties with a continuous impermeable liquid layer. Furthermore, the rational design of liquid surface coatings that gradually wear away or dissipate may be used as a mechanism to control the rate of biosorption of magnesium alloys,<sup>[185]</sup> facilitating the design of resorbable implants or implant parts.<sup>[186–188]</sup>

One essential property of implants is the ability to maintain both the structural integrity and intended function of their surface in the face of abrasion and/or mechanical shear encountered over the weeks, months, or even years that they are in service. Currently, long-term stability is a significant challenge for even the most chemically compatible and surface-energy-matched combinations of substrate and infusing liquid. While for polymer substrates there are some potential solutions to this issue, expanding this ability to harder materials such as metals and ceramics will require clever technological advances. This should include exploring options for creating liquid-infused surfaces on metal implants designed to replace bone. Although a difficult challenge, success here would bring significant rewards in reducing infection and complication rates, in improving patient outcomes, and lowering healthcare costs associated with repeat treatments.

#### 4.5. Tissue Integration and Manipulation

The longest-term use of medical devices often has the goal of reverting the body back to its original healthy state as much as possible, either through the replacement of implant materials with tissue or the integration of tissue within the implant structure. Achieving this aim requires understanding and working with the foreign body response,<sup>[189]</sup> as well as controlling the proliferation of microorganisms, if present. Although still in the early stages, there have already been some provocative results showing how liquid-infused surfaces may alter the foreign body response as well as serve to control infection. In the *in vivo* experiments on a rat implant-associated infection model discussed in Section 4.4,<sup>[35]</sup> the concurrent immune response was also significantly mitigated. In addition to a reduced bacterial load and infection rate, the presence of leukocytes was reduced by 90% on the implant surfaces and by 50% in the surrounding tissue. At 7 days post-treatment, histological results revealed a significant decrease in the width of the fibrous capsule surrounding the implants with infused liquid layers compared to solid controls, as well as significantly reduced levels of the cytokines IL-1 $\beta$  and IL-6 (**Figure 19A**), which indicate the activation level of the inflammatory response. Although this time frame was too short to encompass the full span of capsule formation, the results nevertheless suggest that the presence of a liquid layer was altering the early foreign body host response.

An alternative approach to reducing fibrous capsule formation using infused liquid layers explored central venous catheters coated with a water layer held in place by a continuously-replenished permeable hydrophilic membrane (**Figure 19B**).<sup>[190]</sup> This approach yielded a 92% reduction in protein adhesion, the first step in capsule formation, when used in contact with whole blood under flow. Given that many implants and devices suffer from complications associated with



the formation of fibrous capsules, the use of liquid-infused surfaces to alter both the protein deposition events and immune system functions that result in this aspect of the foreign body response will have widespread impact.

Future work at the intersection of tissue integration and liquid-infused surfaces may also benefit from focusing on designing liquid-infused surfaces that can play an initial functional anti-adhesion role and then revert to a more adhesion-permitting state to allow for the integration of host tissue. For example, the latter may prove particularly useful in designing bone implants that resist bacterial attachment and colonization upon insertion and within a certain period of time after surgery, but lose their liquid-infused character over time to create conditions for the bone tissue ingrowth into the implant surface.<sup>[31]</sup> Alternatively, a model which predicts when droplets associated with an infused liquid layer will overflow surface structures and de-pin from the surface, as well as how this process can be controlled using surfactants,<sup>[191]</sup> may prove useful in the design of dynamic or responsive surfaces that lose their functional liquid layer at a predetermined time or after a particular event.<sup>[31]</sup>

Finally, the manipulation of tissue is of growing interest in both medical and pharmaceutical applications, including the 3D printing of cell-laden structures and the development of new organ-on-a-chip systems. Aspects of liquid-infused surfaces such as their potential use as cell-sheet-release surfaces<sup>[114]</sup> (see Section 3.3) and ability when used as liquid-gated membranes to remove gas bubbles<sup>[98]</sup> (see Section 2.5) from fluids such as 3D bioprinting inks may present interesting new pathways to explore. When combined with the self-replenishing potential offered by liquid-secreting<sup>[72]</sup> and vascularized<sup>[71]</sup> polymers or the multi-functional potential offered by drug-loaded

liquids,<sup>[104,105]</sup> there is great potential to enable new disruptive technologies in the field of tissue manipulation.

## 5. Outlook

Biology's sticky substances, tissues, and microbes are among the most persistent and dangerous forms of surface fouling – with entire response cascades evolved to recognize and take advantage of stable surfaces, they have raised the question of whether it is even possible to design fouling-resistant biomedical devices. While much is left to learn, the work discussed in this review suggests that a fully liquid interface can avoid triggering the responses commonly induced by solid materials, and yet – counterintuitively as a liquid – simultaneously enhance material robustness and versatility. Notably, a wide range of liquid-infused surfaces display unprecedented antifouling performance even with little or no optimization, enabling fouling resistance to be integrated with the diverse demands of surgical instruments, implants, cameras, wound dressings and many other medical materials and devices. Systematic analysis of antifouling behavior as a function of different substrate-liquid combinations will be essential to developing a comprehensive, rational framework for future design, and will also provide new fundamental insight into how numerous parameters – molecular scale mobility, surface tension, viscosity, nano- and microscale mobility, overlayer thickness, and mechanical deformability of the liquid interface, as well as chemistry, elasticity and geometry of the underlying solid – influence whether a biological system ultimately recognizes a stable surface.

At the same time, the exploration of liquid-infused surfaces as antifouling coatings has unexpectedly raised the possibility of a much wider field of biological manipulations using liquid

interfaces. Growing evidence suggests that liquid coatings, rather than making the surface “invisible”, may invoke initial recognition but then prevent or fundamentally alter the downstream responses of microbes and mammalian cells. With the wide range of surface dynamics made possible by the hybrid system, a compelling direction may be the use of the interface as a “liquid tuner” for selecting and controlling specific biological behaviors. Surface chemistry, mechanics, and geometry are known to influence tissue and biofilm development, protein function, and many other processes, but a liquid-infused material presents a unique and versatile tool for modulating the biointerface. For example, a variety of surface parameters can be systematically tailored without disrupting the continuity of the liquid layer, simply by varying the liquid thickness to progressively invoke underlying surface patterns or embedded biomolecules. This suggests not only that antifouling behavior and fine, multifaceted selectivity can be combined in a single surface, but that the liquid interface may introduce opportunities to discover and design previously unimagined biomedical functions.

As a hybrid design is dependent on the interplay between the two components rather than any specific liquid or solid, the most transformative potential of liquid-infused materials may be not as a replacement for current strategies but as a platform for unifying many promising fields and lines of research. This is already beginning to happen, for example with the incorporation of antimicrobial components in the liquid layer to create synergy between physical and biochemical antifouling approaches. The variety of adaptive liquid-infused surface strategies further lend themselves to integration with responsive or bioactive polymers or topography-based manipulation, adding new dimensions to processes ranging from regulated drug delivery to cell fate control. At the same time, a growing class of responsive liquids, functional molecular liquids, and liquid crystals will likely be

influenced by the confinement geometry of the substrate, may have unique surface properties, and can additionally have catalytic or other bioactive functions at the molecular level as well as optical, thermal, and electronic tunability. With numerous degrees of freedom remaining to be explored, liquid-infused materials offer a unique system to integrate and harness these effects.

Ultimately, as water/air purification and other technologies increasingly rely on complex microbial-based surface processes, the insights and design principles discussed in this review may further inspire materials innovations addressing broader healthcare challenges, from hospital air quality to space or deep-sea medicine to environmental and public health.

#### Acknowledgements

The work was supported by the NSF MRSEC award No. DMR-1420570. The authors thank Adrian Arias Palomo for technical editing and helpful advice.

Received: ((will be filled in by the editorial staff))

Revised: ((will be filled in by the editorial staff))

Published online: ((will be filled in by the editorial staff))

## References

- [1] J. R. Bessell, E. Flemming, W. Kunert, G. Buess, *Minim. Invasive Ther. Allied Technol.* **1996**, *5*, 450.
- [2] H. Zhang, M. Chiao, *J. Med. Biol. Eng.* **2015**, *35*, 143.
- [3] R. Romero, C. Schaudinn, J. P. Kusanovic, A. Gorur, F. Gotsch, P. Webster, C.-L. Nhan-Chang, O. Erez, C. J. Kim, J. Espinoza, L. F. Gonçalves, E. Vaisbuch, S. Mazaki-Tovi, S. S. Hassan, J. W. Costerton, *Am. J. Obstet. Gynecol.* **2008**, *198*, 135.e1.
- [4] D. Alves, M. Olívia Pereira, *Biofouling* **2014**, *30*, 483.
- [5] L. M. Hamming, B. Phillip, *Mater. Matters* **2008**, *3*, 52.
- [6] X. Zhang, F. Shi, J. Niu, Y. Jiang, Z. Wang, *J. Mater. Chem.* **2008**, *18*, 621.
- [7] W. Barthlott, C. Neinhuis, *Planta* **1997**, *202*, 1.
- [8] X.-M. Li, D. Reinhoudt, M. Crego-Calama, *Chem. Soc. Rev.* **2007**, *36*, 1350.
- [9] T. Sun, L. Feng, X. Gao, L. Jiang, **2005**, *38*, 644.
- [10] S. Chen, L. Li, C. Zhao, J. Zheng, *Polymer (Guildf)*. **2010**, *51*, 5283.
- [11] M. Berglin, M. Andersson, A. Sellborn, H. Elwing, *Biomaterials* **2004**, *25*, 4581.
- [12] I. Banerjee, R. C. Pangule, R. S. Kane, *Adv. Mater.* **2011**, *23*, 690.
- [13] R. S. Friedlander, N. Vogel, J. Aizenberg, *Langmuir* **2015**, *31*, 6137.

- [14] R. S. Friedlander, H. Vlamakis, P. Kim, M. Khan, R. Kolter, J. Aizenberg, *Proc. Natl. Acad. Sci.* **2013**, *110*, 5624.
- [15] G. B. Sigal, M. Mrksich, G. M. Whitesides, *J. Am. Chem. Soc.* **1998**, *120*, 3464.
- [16] E. Namati, J. Thiesse, J. De Ryk, G. McLennan, *Am. J. Respir. Cell Mol. Biol.* **2008**, *38*, 572.
- [17] H. F. Bohn, W. Federle, *Proc. Natl. Acad. Sci. U. S. A.* **2004**, *101*, 14138.
- [18] D. Labonte, W. Federle, *Soft Matter* **2015**, *11*, 8661.
- [19] J. H. Dirks, W. Federle, *J. R. Soc. Interface* **2011**, *8*, 952.
- [20] J.-H. Dirks, C. J. Clemente, W. Federle, *J. R. Soc. Interface* **2010**, *7*, 587.
- [21] L. Gaume, P. Perret, E. Gorb, S. Gorb, J. J. Labat, N. Rowe, *Arthropod Struct. Dev.* **2004**, *33*, 103.
- [22] T.-S. Wong, S. H. Kang, S. K. Y. Tang, E. J. Smythe, B. D. Hatton, A. Grinthal, J. Aizenberg, *Nature* **2011**, *477*, 443.
- [23] J. Aizenberg, M. Aizenberg, S. H. Kang, T. S. Wong, P. Kim, *Slippery Surfaces with High Pressure Stability, Optical Transparency, and Self-Healing Characteristics*, **2015**, US Patent 9121306 B2.
- [24] M. Cao, D. Guo, C. Yu, K. Li, M. Liu, L. Jiang, *ACS Appl. Mater. Interfaces* **2016**, *8*, 3615.
- [25] D. Quéré, *Reports Prog. Phys.* **2005**, *68*, 2495.
- [26] A. Lafuma, D. Quéré, *EPL* **2011**, *96*, 56001.

- [27] D. Daniel, J. V. I. Timonen, R. Li, S. J. Velling, J. Aizenberg, *Nat. Phys.* **2017**, *13*, 1020.
- [28] P. Kim, T.-S. Wong, J. Alvarenga, M. J. Kreder, W. E. Adorno-Martinez, J. Aizenberg, *ACS Nano* **2012**, *6*, 6569.
- [29] S. B. Subramanyam, K. Rykaczewski, K. K. Varanasi, *Langmuir* **2013**, *29*, 13414.
- [30] L. E. Vaaler, *Impregnated Porous Condenser Surfaces*, **1959**, US Patent 2919115 A.
- [31] J. Aizenberg, M. Aizenberg, B. Hatton, W. Wang, X. Yao, *Dynamic and Switchable Slippery Surfaces*, **2017**, US Patent 9683197 B2.
- [32] J. J. Bauer, B. A. Salky, I. M. Gelernt, I. Kreel, *Ann. Surg.* **1987**, *206*, 765.
- [33] C. N. Brown, J. G. Finch, *Ann. R. Coll. Surg. Engl.* **2010**, *92*, 272.
- [34] W. Becker, C. Dahlin, B. E. Becker, U. Lekholm, D. van Steenberghe, K. Higuchi, C. Kultje, *Int. J. Oral Maxillofac. Implants* **1994**, *9*, 31.
- [35] J. Chen, C. Howell, C. A. Haller, M. S. Patel, P. Ayala, K. A. Moravec, E. Dai, L. Liu, I. Sotiri, M. Aizenberg, J. Aizenberg, E. L. Chaikof, *Biomaterials* **2017**, *113*, 80.
- [36] J. Yong, J. Huo, Q. Yang, F. Chen, Y. Fang, X. Wu, L. Liu, X. Lu, J. Zhang, X. Hou, *Adv. Mater. Interfaces* **2018**, 1701479.
- [37] D. C. Leslie, A. Waterhouse, J. B. Berthet, T. M. Valentin, A. L. Watters, A. Jain, P. Kim, B. D. Hatton, A. Nedder, K. Donovan, E. H. Super, C. Howell, C. P. Johnson, T. L. Vu, D. E. Bolgen, S. Rifai, A. R. Hansen, M. Aizenberg, M. Super, J. Aizenberg, D. E. Ingber, *Nat. Biotechnol.* **2014**, *32*, 1134.

- [38] K. Doll, E. Fadeeva, J. Schaeske, T. Ehmke, A. Winkel, A. Heisterkamp, B. N. Chichkov, M. Stiesch, N. S. Stumpp, *ACS Appl. Mater. Interfaces* **2017**, *9*, 9359.
- [39] P. Wang, Z. Lu, D. Zhang, *Corros. Sci.* **2015**, *93*, 159.
- [40] R. Togasawa, M. Tenjimabayashi, T. Matsubayashi, T. Moriya, K. Manabe, S. Shiratori, *ACS Appl. Mater. Interfaces* **2018**, *10*, 4198.
- [41] U. Manna, D. M. Lynn, *Adv. Mater.* **2015**, *27*, 3007.
- [42] H. Liu, P. Zhang, M. Liu, S. Wang, L. Jiang, *Adv. Mater.* **2013**, *25*, 4477.
- [43] A. B. Tesler, P. Kim, S. Kolle, C. Howell, O. Ahanotu, J. Aizenberg, *Nat. Commun.* **2015**, *6*, 8649.
- [44] J. L. Yin, M. L. Mei, Q. L. Li, R. Xia, Z. H. Zhang, C. H. Chu, *Sci. Rep.* **2016**, *6*, 1.
- [45] P. Wang, D. Zhang, S. Sun, T. Li, Y. Sun, *ACS Appl. Mater. Interfaces* **2017**, *9*, 972.
- [46] S. Sunny, G. Cheng, D. Daniel, P. Lo, S. Ochoa, C. Howell, N. Vogel, A. Majid, J. Aizenberg, *Proc. Natl. Acad. Sci. U. S. A.* **2016**, *113*, 11676.
- [47] C. Shillingford, N. MacCallum, T.-S. Wong, P. Kim, J. Aizenberg, *Nanotechnology* **2014**, *25*, 014019.
- [48] V. G. Damle, A. Tummala, S. Chandrashekar, C. Kido, A. Roopesh, X. Sun, K. Doudrick, J. Chinn, J. R. Lee, T. P. Burgin, K. Rykaczewski, *ACS Appl. Mater. Interfaces* **2015**, *7*, 4224.
- [49] A. C. Glavan, R. V. Martinez, A. B. Subramaniam, H. J. Yoon, R. M. D. Nunes, H. Lange, M. M. Thuo, G. M. Whitesides, *Adv. Funct. Mater.* **2014**, *24*, 60.



- [50] H. Guo, P. Fuchs, K. Casdorff, B. Michen, M. Chanana, H. Hagendorfer, Y. E. Romanyuk, I. Burgert, *Adv. Mater. Interfaces* **2017**, *4*, 1600289.
- [51] K. Manabe, K. H. Kyung, S. Shiratori, *ACS Appl. Mater. Interfaces* **2015**, *7*, 4763.
- [52] S. Sunny, N. Vogel, C. Howell, T. L. Vu, J. Aizenberg, *Adv. Funct. Mater.* **2014**, *24*, 6658.
- [53] S. Yuan, Z. Li, L. Song, H. Shi, S. Luan, J. Yin, *ACS Appl. Mater. Interfaces* **2016**, *8*, 21214.
- [54] P. Kim, M. J. Kreder, J. Alvarenga, J. Aizenberg, *Nano Lett.* **2013**, *13*, 1793.
- [55] C. Howell, T. L. Vu, C. P. Johnson, X. Hou, O. Ahanotu, J. Alvarenga, D. C. Leslie, O. Uzun, A. Waterhouse, P. Kim, M. Super, M. Aizenberg, D. E. Ingber, J. Aizenberg, *Chem. Mater.* **2015**, *27*, 1792.
- [56] R. Togasawa, F. Ohnuki, S. Shiratori, **2018**, *1*, 1758.
- [57] P. A. Levkin, F. Svec, J. M. J. Fréchet, *Adv. Funct. Mater.* **2009**, *19*, 1993.
- [58] J. Li, T. Kleintschek, A. Rieder, Y. Cheng, T. Baumbach, U. Obst, T. Schwartz, P. A. Levkin, *ACS Appl. Mater. Interfaces* **2013**, *5*, 6704.
- [59] I. Okada, S. Shiratori, *ACS Appl. Mater. Interfaces* **2014**, *6*, 1502.
- [60] S. Yuan, S. Luan, S. Yan, H. Shi, J. Yin, *ACS Appl. Mater. Interfaces* **2015**, *7*, 19466.
- [61] T. Hang, H.-J. Chen, C. Yang, S. Xiao, G. Liu, D. Lin, J. Tao, J. Wu, B. Yang, X. Xie, *RSC Adv.* **2017**, *7*, 55812.
- [62] S. Zouaghi, T. Six, S. Bellayer, S. Moradi, S. G. Hatzikiriakos, T. Dargent, V. Thomy, Y. Coffinier,

- C. André, G. Delaplace, M. Jimenez, *ACS Appl. Mater. Interfaces* **2017**, 9, 26565.
- [63] J. Yong, F. Chen, Q. Yang, Y. Fang, J. Huo, J. Zhang, X. Hou, *Adv. Mater. Interfaces* **2017**, 4, 1.
- [64] P. Zhang, H. Chen, L. Zhang, T. Ran, D. Zhang, *Appl. Surf. Sci.* **2015**, 355, 1083.
- [65] N. Vogel, R. A. Belisle, B. D. Hatton, T.-S. Wong, J. Aizenberg, *Nat. Commun.* **2013**, 4, 2167.
- [66] J. Aizenberg, N. Vogel, *Slippery Liquid-Infused Porous Surfaces Having Improved Stability*, **2017**, US Patent 9630224 B2.
- [67] M. Tenjimbayashi, R. Togasawa, K. Manabe, T. Matsubayashi, T. Moriya, M. Komine, S. Shiratori, *Adv. Funct. Mater.* **2016**, 26, 6693.
- [68] I. Sotiri, J. C. Overton, A. Waterhouse, C. Howell, *Exp. Biol. Med.* **2016**, 241, 909.
- [69] D. Daniel, J. V. I. Timonen, R. Li, S. J. Velling, J. Aizenberg, *Nat. Phys.* **2017**, 13, 1020.
- [70] M. Badv, I. H. Jaffer, J. I. Weitz, T. F. Didar, *Sci. Rep.* **2017**, 7, 1.
- [71] C. Howell, T. L. Vu, J. J. Lin, S. Kolle, N. Juthani, E. Watson, J. C. Weaver, J. Alvarenga, J. Aizenberg, *ACS Appl. Mater. Interfaces* **2014**, 6, 13299.
- [72] J. Cui, D. Daniel, A. Grinthal, K. Lin, J. Aizenberg, *Nat. Mater.* **2015**, 14, 790.
- [73] C. Urata, G. J. Dunderdale, M. W. England, A. Hozumi, *J. Mater. Chem. A* **2015**, 3, 12626.
- [74] X. Yao, S. S. Dunn, P. Kim, M. Duffy, J. Alvarenga, J. Aizenberg, *Angew. Chem. Int. Ed. Engl.* **2014**, 53, 4418.
- [75] J. Aizenberg, M. Aizenberg, J. Cui, S. Dunn, B. D. Hatton, C. Howell, P. Kim, T.-S. Wong, X. Yao,

*Slippery Self-Lubricating Polymer Surfaces*, **2018**, US Patent 9963597 B2.

- [76] Q. Wei, C. Schlaich, S. Prévost, A. Schulz, C. Böttcher, M. Gradzielski, Z. Qi, R. Haag, C. A. Schalley, *Adv. Mater.* **2014**, *26*, 7358.
- [77] H. Zhao, J. Xu, G. Jing, L. O. Prieto-López, X. Deng, J. Cui, *Angew. Chemie Int. Ed.* **2016**, *55*, 10681.
- [78] J. Lv, X. Yao, Y. Zheng, J. Wang, L. Jiang, *Adv. Mater.* **2017**, *29*, 1703032.
- [79] C. I. Castro, J. C. Briceno, *Artif. Organs* **2010**, *34*, 622.
- [80] S. G. Kramer, D. Hwang, G. A. Peyman, J. A. Schulman, B. Sullivan, *Surv. Ophthalmol.* **1995**, *39*, 375.
- [81] M. S. Figueroa, D. R. Casas, *Biomed Res. Int.* **2014**, 907816, 1.
- [82] U. Spandau, M. Pavlidis, *27-Gauge Vitrectomy: Minimal Sclerotomies for Maximal Results*, Springer International Publishing, Heidelberg, **2015**.
- [83] R. S. Narins, K. Beer, *Plast. Reconstr. Surg.* **2006**, *118*, 77S.
- [84] M. Smiglak, J. M. Pringle, X. Lu, L. Han, S. Zhang, H. Gao, D. R. MacFarlane, R. D. Rogers, *Chem. Commun.* **2014**, *50*, 9228.
- [85] Y. Ding, J. Zhang, X. Zhang, Y. Zhou, S. Wang, H. Liu, L. Jiang, *Adv. Mater. Interfaces* **2015**, *2*, 2.
- [86] Y. Galvan, K. R. Phillips, M. Haumann, P. Wasserscheid, R. Zarraga, N. Vogel, *Langmuir* **2018**, DOI: 10.1021/acs.langmuir.7b03993.

- [87] S. Nishioka, M. Tenjimabayashi, K. Manabe, T. Matsubayashi, K. Suwabe, K. Tsukada, S. Shiratori, *RSC Adv.* **2016**, *6*, 47579.
- [88] S. Sunny, No Harm No Foul: Coating for Medical Applications (Doctoral Dissertation), Harvard University, **2017**.
- [89] J. D. Smith, R. Dhiman, S. Anand, E. Reza-Garduno, R. E. Cohen, G. H. McKinley, K. K. Varanasi, *Soft Matter* **2013**, *9*, 1772.
- [90] F. Schellenberger, J. Xie, N. Encinas, A. Hardy, M. Klapper, P. Papadopoulos, H.-J. Butt, D. Vollmer, *Soft Matter* **2015**, *11*, 7617.
- [91] S. Sett, X. Yan, G. Barac, L. Bolton, N. Miljkovic, *ACS Appl. Mater. Interfaces* **2017**, *9*, 36400.
- [92] M. Tress, S. Karpitschka, P. Papadopoulos, J. H. Snoeijer, D. Vollmer, H.-J. Butt, *Soft Matter* **2017**, *13*, 3760.
- [93] J. S. Wexler, I. Jacobi, H. A. Stone, *Phys. Rev. Lett.* **2015**, *114*, 1.
- [94] D. J. Preston, Y. Song, Z. Lu, D. S. Antao, E. N. Wang, *ACS Appl. Mater. Interfaces* **2017**, *9*, 42383.
- [95] D. Truzzolillo, S. Mora, C. Dupas, L. Cipelletti, *Phys. Rev. X* **2016**, *6*, 1.
- [96] X. Yao, Y. Hu, A. Grinthal, T.-S. Wong, L. Mahadevan, J. Aizenberg, *Nat. Mater.* **2013**, *12*, 529.
- [97] C. Liu, H. Ding, Z. Wu, B. Gao, F. Fu, L. Shang, Z. Gu, Y. Zhao, *Adv. Funct. Mater.* **2016**, *26*, 7937.

- [98] X. Hou, Y. Hu, A. Grinthal, M. Khan, J. Aizenberg, *Nature* **2015**, 519, 70.
- [99] Z. Sheng, H. Wang, Y. Tang, M. Wang, L. Huang, L. Min, H. Meng, S. Chen, L. Jiang, X. Hou, *Sci. Adv.* **2018**, 4, 1.
- [100] J. C. Overton, A. Weigang, C. Howell, *J. Memb. Sci.* **2017**, 539, 257.
- [101] K. Manabe, T. Matsubayashi, M. Tenjimbayashi, T. Moriya, Y. Tsuge, K. H. Kyung, S. Shiratori, *ACS Nano* **2016**, 10, 9387.
- [102] L. Wang, L. Heng, L. Jiang, *ACS Appl. Mater. interfaces Interfaces* **2018**, 10, 7442.
- [103] X. Yao, J. Ju, S. Yang, J. Wang, L. Jiang, *Adv. Mater.* **2014**, 26, 1895.
- [104] U. Manna, N. Raman, M. A. Welsh, Y. M. Zayas-Gonzalez, H. E. Blackwell, S. P. Palecek, D. M. Lynn, *Adv. Funct. Mater.* **2016**, 3599.
- [105] M. J. Kratochvil, M. A. Welsh, U. Manna, B. J. Ortiz, H. E. Blackwell, D. M. Lynn, *ACS Infect. Dis.* **2016**, 2, 509.
- [106] M. J. Goudie, J. Pant, H. Handa, *Sci. Rep.* **2017**, 7, 1.
- [107] H. Zhao, J. Xu, G. Jing, L. O. Prieto-López, X. Deng, J. Cui, *Angew. Chemie - Int. Ed.* **2016**, 55, 10681.
- [108] M. J. Kreder, J. Alvarenga, P. Kim, J. Aizenberg, *Nat. Rev. Mater.* **2016**, 1, 15003.
- [109] S. B. Subramanyam, G. Azimi, K. K. Varanasi, *Adv. Mater. Interfaces* **2014**, 1, 1.
- [110] J. Wang, K. Kato, A. P. Blois, T. S. Wong, *ACS Appl. Mater. Interfaces* **2016**, 8, 8265.

- [111] J. Aizenberg, B. D. Hatton, D. E. Ingber, M. Super, T.-S. Wong, *Slippery Liquid-Infused Porous Surfaces and Biological Applications Thereof*, **2018**, US 9932484 B2.
- [112] J. Aizenberg, T. S. Wong, B. Hatton, *Selective Wetting and Transport Surfaces*, **2014**, US Patent Application WO2014012078 A2.
- [113] K. Sasaki, M. Tenjimbayashi, K. Manabe, S. Shiratori, *ACS Appl. Mater. Interfaces* **2016**, *8*, 651.
- [114] N. Juthani, C. Howell, H. Ledoux, I. Sotiri, S. Kelso, Y. Kovalenko, A. Tajik, T. L. Vu, J. J. Lin, A. Sutton, J. Aizenberg, *Sci. Rep.* **2016**, *6*, 26109.
- [115] J. B. Boreyko, G. Polizos, P. G. Datskos, S. A. Sarles, C. P. Collier, *Proc. Natl. Acad. Sci.* **2014**, *111*, 7588.
- [116] L. He, A. F. Dexter, A. P. J. Middelberg, *Chem. Eng. Sci.* **2006**, *61*, 989.
- [117] D. B. Jones, A. P. J. Middelberg, *AIChE J.* **2003**, *49*, 1533.
- [118] D. B. Jones, A. P. J. Middelberg, *Langmuir* **2002**, *18*, 5585.
- [119] H. González-Navarro, L. Braco, *Biotechnol. Bioeng.* **1998**, *59*, 122.
- [120] A. J. J. Straathof, *Biotechnol. Bioeng.* **2003**, *83*, 371.
- [121] K. Piradashvili, E. M. Alexandrino, F. R. Wurm, K. Landfester, *Chem. Rev.* **2015**, *116*, 2141.
- [122] J. Geng, C. Beloin, J. M. Ghigo, N. Henry, *PLoS One* **2014**, *9*, 1.
- [123] R. Belas, *Trends Microbiol.* **2014**, *22*, 517.
- [124] L. McCarter, M. Hilmen, M. Silverman, *Cell* **1988**, *54*, 345.

- [125] S. L. Kuchma, G. A. O'Toole, *Curr. Opin. Biotechnol.* **2000**, *11*, 429.
- [126] M. Whiteley, S. P. Diggle, E. P. Greenberg, *Nature* **2017**, *551*, 313.
- [127] S. S. Branda, A. Vik, L. Friedman, R. Kolter, *Trends Microbiol.* **2005**, *13*, 20.
- [128] A. Persat, C. D. Nadell, M. K. Kim, F. Ingremeau, A. Sityaporn, K. Drescher, N. S. Wingreen, B. L. Bassler, Z. Gitai, H. A. Stone, *Cell* **2015**, *161*, 988.
- [129] A. Persat, H. A. Stone, Z. Gitai, *Nat. Commun.* **2014**, *5*, 3824.
- [130] P. S. Stewart, J. William Costerton, *Lancet* **2001**, *358*, 135.
- [131] K. Bazaka, M. V Jacob, R. J. Crawford, E. P. Ivanova, *Acta Biomater.* **2011**, *7*, 2015.
- [132] P. Kingshott, J. Wei, D. Bagge-Ravn, N. Gadegaard, L. Gram, *Langmuir* **2003**, *19*, 6912.
- [133] S. T. Reddy, K. K. Chung, C. J. McDaniel, R. O. Darouiche, J. Landman, A. B. Brennan, *J. Endourol.* **2011**, *25*, 1547.
- [134] W. M. Dunne, *Clin. Microbiol. Rev.* **2002**, *15*, 155.
- [135] R. Laxminarayan, A. Duse, C. Wattal, A. K. M. Zaidi, H. F. L. Wertheim, N. Sumpradit, E. Vlieghe, G. L. Hara, I. M. Gould, H. Goossens, C. Greko, A. D. So, M. Bigdeli, G. Tomson, W. Woodhouse, E. Ombaka, A. Q. Peralta, F. N. Qamar, F. Mir, S. Kariuki, Z. A. Bhutta, A. Coates, R. Bergstrom, G. D. Wright, E. D. Brown, O. Cars, *Lancet Infect. Dis.* **2013**, *13*, 1057.
- [136] A. K. Epstein, T.-S. Wong, R. A. Belisle, E. M. Boggs, J. Aizenberg, *Proc. Natl. Acad. Sci. U. S. A.* **2012**, *109*, 13182.

- [137] Y. Kovalenko, I. Sotiri, J. V. I. Timonen, J. C. Overton, G. Holmes, J. Aizenberg, C. Howell, *Adv. Healthc. Mater.* **2017**, 1600948.
- [138] N. MacCallum, C. Howell, P. Kim, D. Sun, R. Friedlander, J. Ranisau, O. Ahanotu, J. J. Lin, A. Vena, B. Hatton, T. S. Wong, J. Aizenberg, *ACS Biomater. Sci. Eng.* **2015**, 1, 43.
- [139] J. Jiang, H. Zhang, W. He, T. Li, H. Li, P. Liu, M. Liu, Z. Wang, Z. Wang, X. Yao, *ACS Appl. Mater. Interfaces* **2017**, 9, 6599.
- [140] L. A. Pratt, R. Kolter, *Mol. Microbiol.* **1998**, 30, 285.
- [141] K. L. Van Dellen, L. Houot, P. I. Watnick, *J. Bacteriol.* **2008**, 190, 8185.
- [142] C. J. Gode-Potratz, R. J. Kustus, P. J. Breheny, D. S. Weiss, L. L. McCarter, *Mol. Microbiol.* **2011**, 79, 240.
- [143] R. Belas, R. Suvanasuthi, *J. Bacteriol.* **2005**, 187, 6789.
- [144] Y. Y. Lee, J. Patellis, R. Belas, *J. Bacteriol.* **2013**, 195, 823.
- [145] D. Daniel, M. N. Mankin, R. A. Belisle, T. S. Wong, J. Aizenberg, *Appl. Phys. Lett.* **2013**, 102, 231603.
- [146] R. Van Houdt, C. W. Michiels, *J. Appl. Microbiol.* **2010**, 109, 1117.
- [147] E. Z. Ron, E. Rosenberg, *Curr. Opin. Biotechnol.* **2002**, 13, 249.
- [148] M. Katsikogianni, Y. F. Missirlis, *Eur. Cell. Mater.* **2004**, 8, 37.
- [149] E. Rosenberg, E. Z. Ron, *Appl. Microbiol. Biotechnol.* **1999**, 52, 154.



- [150] T. R. Neu, *Microbiol. Rev.* **1996**, *60*, 151.
- [151] P. A. Rühs, L. Böcker, R. F. Inglis, P. Fischer, *Colloids Surfaces B Biointerfaces* **2014**, *117*, 174.
- [152] M. Rosenberg, *Crit. Rev. Microbiol.* **1991**, *18*, 159.
- [153] C. Howell, T. L. Vu, J. J. Lin, S. Kolle, N. Juthani, E. Watson, J. C. Weaver, J. Alvarenga, J. Aizenberg, *ACS Appl. Mater. Interfaces* **2014**, *6*, 13299.
- [154] J. Bruchmann, I. Pini, T. S. Gill, T. Schwartz, P. A. Levkin, *Adv. Healthc. Mater.* **2017**, *6*, 1601082.
- [155] W. Shi, T. Xu, L.-P. Xu, Y. Chen, Y. Wen, X. Zhang, S. Wang, *Nanoscale* **2016**, *8*, 18612.
- [156] C. Schlaich, Y. Fan, P. Dey, J. Cui, Q. Wei, R. Haag, X. Deng, *Adv. Mater. Interfaces* **2018**, 1701536.
- [157] E. Ueda, P. A. Levkin, *Adv. Healthc. Mater.* **2013**, *2*, 1425.
- [158] J. Kamei, H. Yabu, *Adv. Funct. Mater.* **2015**, *25*, 4195.
- [159] P. Che, L. Heng, L. Jiang, *Adv. Funct. Mater.* **2017**, *27*, 1.
- [160] J. T. Luo, N. R. Gerald, J. H. Guan, G. McHale, G. G. Wells, Y. Q. Fu, *Phys. Rev. Appl.* **2017**, *7*, 1.
- [161] Y. Zheng, J. Cheng, C. Zhou, H. Xing, X. Wen, P. Pi, S. Xu, *Langmuir* **2017**, *33*, 4172.
- [162] X. Hou, J. Li, A. B. Tesler, Y. Yao, M. Wang, L. Min, Z. Sheng, J. Aizenberg, *Nat. Commun.* **2018**, *9*, 733.
- [163] S. Yang, X. Dai, B. B. Stogin, T.-S. Wong, *Proc. Natl. Acad. Sci.* **2015**, *2015*, 201518980.

- [164] K. Fukada, N. Kawamura, S. Shiratori, *Anal. Chem.* **2017**, *89*, 10391.
- [165] D. S. Miller, N. L. Abbott, *Soft Matter* **2013**, *9*, 374.
- [166] S. Zhou, A. Sokolov, O. D. Lavrentovich, I. S. Aranson, *Proc. Natl. Acad. Sci.* **2014**, *111*, 1265.
- [167] K. Liu, C. Ma, R. Göstl, L. Zhang, A. Herrmann, *Acc. Chem. Res.* **2017**, *50*, 1212.
- [168] Y. Li, J. John, K. W. Kolewe, J. D. Schiffman, K. R. Carter, *ACS Appl. Mater. Interfaces* **2015**, *7*, 23439.
- [169] P. Zhang, H. Chen, L. Zhang, D. Zhang, *Appl. Surf. Sci.* **2016**, *385*, 249.
- [170] J. Abe, M. Tenjimbayashi, S. Shiratori, *RSC Adv.* **2016**, *6*, 38018.
- [171] J. Guo, W. Fang, A. Welle, W. Feng, I. Filpponen, O. J. Rojas, P. A. Levkin, *ACS Appl. Mater. Interfaces* **2016**, *8*, 34115.
- [172] M. Tenjimbayashi, J.-Y. Park, J. Muto, Y. Kobayashi, R. Yoshikawa, Y. Monnai, S. Shiratori, *ACS Biomater. Sci. Eng.* **2018**, *4*, 1871.
- [173] *Infection: Prevention and Control of Healthcare-Associated Infections in Primary and Community Care*, National Clinical Guideline Center, London, **2012**.
- [174] S. Galloway, A. Bodenham, *Br. J. Anaesth.* **2004**, *92*, 722.
- [175] H. Al-Hazmi, *Res. Reports Urol.* **2015**, *7*, 41.
- [176] J. L. Baskin, C. H. Pui, U. Reiss, J. A. Wilimas, M. L. Metzger, R. C. Ribeiro, S. C. Howard, *Lancet* **2009**, *374*, 159.

- [177] Y. Tsuge, T. Moriya, Y. Moriyama, Y. Tokura, S. Shiratori, *ACS Appl. Mater. Interfaces* **2017**, 9, 15122.
- [178] S. Marin, G. Mihail Vlasceanu, R. Elena Tiplea, I. Raluca Bucur, M. Lemnaru, M. Minodora Marin, A. Mihai Grumezescu, *Curr. Top. Med. Chem.* **2015**, 15, 1596.
- [179] R. A. van Hulst, J. Klein, B. Lachmann, *Clin. Physiol. Funct. Imaging* **2003**, 23, 237.
- [180] B. D. Ratner, A. Hoffman, F. Schoen, J. Lemons, Eds. , *Biomaterials Science 3rd Edition: An Introduction to Materials in Medicine*, Academic Press, Waltham, MA, **2013**.
- [181] Y. Yan, A. Neville, D. Dowson, *Proc. Inst. Mech. Eng. Part H* **2006**, 220, 173.
- [182] D. C. Hansen, *Electrochem. Soc. Interface* **2008**, 17, 31.
- [183] S. Sun, P. Wang, D. Zhang, *Corros. Sci. Prot. Technol.* **2016**, 28, 1.
- [184] M. Tenjimbayashi, S. Nishioka, Y. Kobayashi, K. Kawase, J. Li, J. Abe, S. Shiratori, *Langmuir* **2018**, 34, 1386.
- [185] N. T. Kirkland, J. Lespagnol, N. Birbilis, M. P. Staiger, *Corros. Sci.* **2010**, 52, 287.
- [186] D. H. Kim, J. Viventi, J. J. Amsden, J. Xiao, L. Vigeland, Y. S. Kim, J. A. Blanco, B. Panilaitis, E. S. Frechette, D. Contreras, D. L. Kaplan, F. G. Omenetto, Y. Huang, K. C. Hwang, M. R. Zakin, B. Litt, J. A. Rogers, *Nat. Mater.* **2010**, 9, 1.
- [187] S.-W. Hwang, H. Tao, D.-H. Kim, H. Cheng, J.-K. Song, E. Rill, K. J. Yu, A. Ameen, R. Li, Y. Su, M. Yang, D. L. Kaplan, M. R. Zakin, M. J. Slepian, Y. Huang, F. G. Omenetto, J. A. Rogers, *Science* (80-. ). **2012**, 337, 1640.

- [188] S. W. Hwang, G. Park, C. Edwards, E. A. Corbin, S. K. Kang, H. Cheng, J. K. Song, J. H. Kim, S. Yu, J. Ng, J. E. Lee, J. Kim, C. Yee, B. Bhaduri, F. G. Omennetto, Y. Huang, R. Bashir, L. Goddard, G. Popescu, K. M. Lee, J. A. Rogers, *ACS Nano* **2014**, *8*, 5843.
- [189] J. M. Anderson, A. Rodriguez, D. T. Chang, *Semin. Immunol.* **2008**, *20*, 86.
- [190] D. W. Sutherland, X. Zhang, J. L. Charest, *Artif. Organs* **2017**, *41*, E155.
- [191] I. Jacobi, J. S. Wexler, H. A. Stone, *Phys. Fluids* **2015**, *27*, DOI 10.1063/1.4927538.
- [192] X. C. Chen, K. F. Ren, J. Wang, W. X. Lei, J. Ji, *ACS Appl. Mater. Interfaces* **2016**, *9*, 1959.

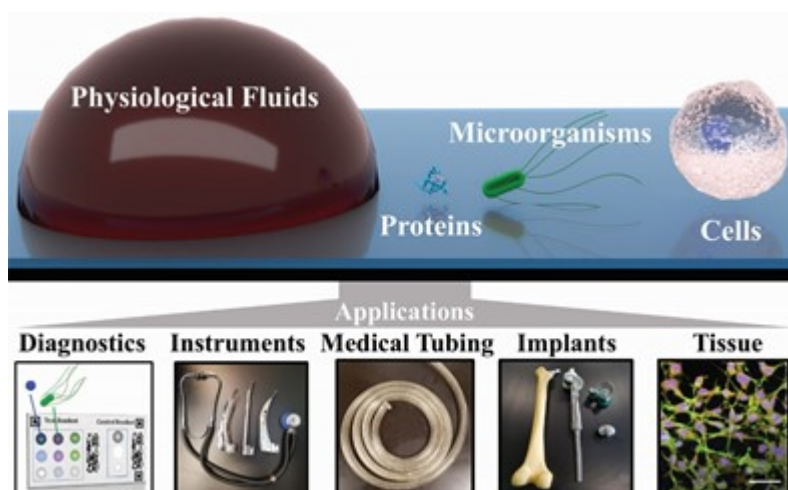


Figure 1. Applications of liquid-infused materials in medicine.

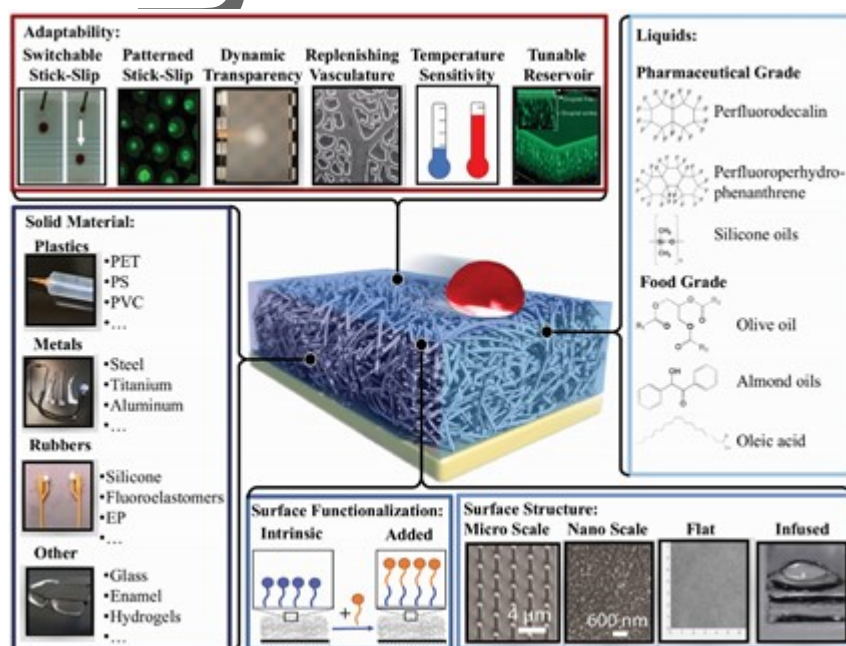
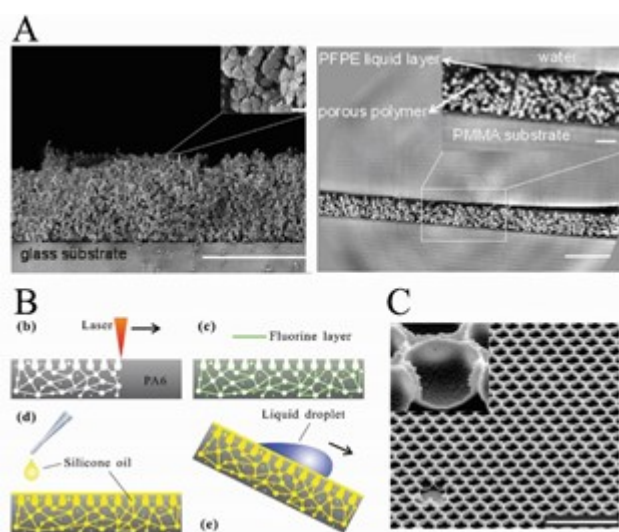
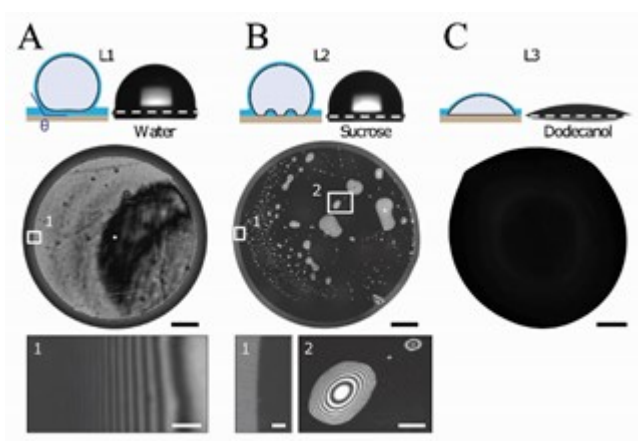


Figure 2. Schematic of the tunable properties of liquid-infused surfaces.



**Figure 3.** Representative types of solid surfaces used to create liquid layers. A) Left: Cross section (scale bar 100  $\mu\text{m}$ ) and surface (inset, scale bar 2  $\mu\text{m}$ ) SEM micrographs showing the morphology of the porous structure of the infused polymer surface. Right: Reconstructed X-ray propagation phase contrast tomography image showing the cross section of the surface under water. The liquid layer is visible on the surface of the porous polymer. Scale bar: 100  $\mu\text{m}$  in the image and 20  $\mu\text{m}$  in the inset. Reproduced with permission.<sup>[58]</sup> Copyright 2013, American Chemical Society. B) b) Formation of 3D porous microstructures through femtosecond laser ablation. c) Modifying the porous substrate with a fluorine layer. d) Infusion of silicone oil. e) Schematic illustration of liquid droplet sliding down the as-prepared SLIPS. Reproduced with permission.<sup>[63]</sup> Copyright 2017, WILEY-VCH Verlag GmbH & Co. C) SEM image of an open-cell structure taken at an angle of 45° showing high regularity and structural details of the nanopore arrays. Reproduced with permission.<sup>[65]</sup> Copyright 2013, Macmillan Publishers Limited.



**Figure 4.** Equilibrium states of a liquid layer sandwiched between a droplet and a solid surface. A) L1: stable lubricant film (silicone oil) beneath a water droplet (0.1 mm scale bar), with inset 1 (10  $\mu\text{m}$  scale bar) showing the absence of a contact line. B) L2: lubricant film is unstable beneath 60 wt % sucrose solution and forms discrete pockets (0.3 mm scale bar). Inset 1 (15  $\mu\text{m}$  scale bar) shows the three-phase contact line, while inset 2 (40  $\mu\text{m}$  scale bar) is a zoomed-in image of the lubricant pockets. C) L3: lubricant is completely displaced from beneath a dodecanol droplet (0.1 mm scale bar). Reproduced with permission.<sup>[69]</sup> Copyright 2017, Macmillan Publishers Limited.

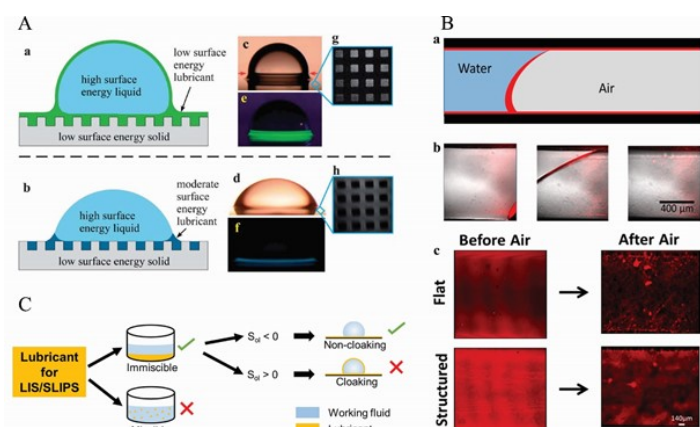


**Figure 5.** Formation and effects of droplet cloaking layers on liquid-infused surfaces. A) Schematic diagrams of a liquid droplet placed on a textured surface with an infusing liquid that a) wets the solid completely, and b) wets the solid with a non-zero contact angle in the presence of air and the droplet liquid. c,d) Photographs of a water droplet on a silicon micro-post surface coated with octadecyltrichlorosilane and infused with c) silicone oil and d) ionic liquid, respectively. e,f) Photograph of a water droplet under UV illumination when a fluorescent dye was dissolved in silicone oil and ionic liquid. g,h) Laser confocal fluorescence microscopy images of the infused texture. Reproduced with permission.<sup>[89]</sup> Copyright 2013, Royal Society of Chemistry. B) Conditions for effective selection of lubricant in designing stable liquid-infused surfaces. Reproduced with permission.<sup>[91]</sup> 2017, American Chemical Society. C) Schematic (a) and composite fluorescent-light microscopy image (b) of a microchannel as the air/water interface passes (top-down view). The interface shows a distinct coating of the lubricant, as would be expected due to the formation of a wrapping layer. c) Top-down views of the flat and structured surfaces coated with a perfluorinated liquid before and after passage of the air/water interface. Reproduced with permission.<sup>[55]</sup> Copyright 2015, American Chemical Society.



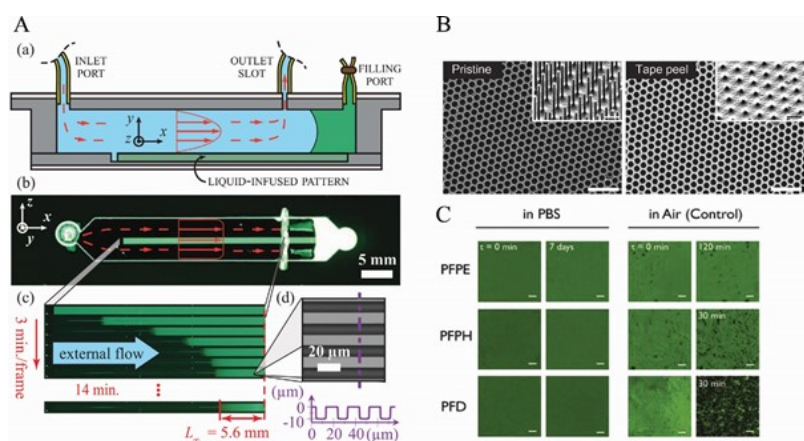


**Figure 6.** Stability of liquid-infused surfaces exposed to flow, damage, and evaporation. A) a) Cross section of the microfluidic flow cell showing the configuration at the beginning of an experiment. Distances in the  $y$  direction are exaggerated. The aqueous solution (blue) flows in the left inlet and out the first (slot-shaped) outlet. The grooves are filled with oil (green), and connect to the reservoir of oil at the flow cell terminus. b) This planform view shows the entire device before drainage commences. Low viscosity oil fills the 50 longitudinal grooves at the center of the device and fluoresces green. c) Snapshots of a sample shear-driven drainage experiment subject to an aqueous flow of  $Q = 2 \text{ mL min}^{-1}$  ( $\tau_{yx} = 5.2 \text{ Pa}$ ). d) Micrograph of the silicon wafer micropattern that is used to mold the grooves, including the surface profile (purple). Grooves appear dark gray and walls appear light gray. Reproduced with permission.<sup>[93]</sup> Copyright 2015, American Physical Society. B) Mechanical stability of the closed-cell, inverse monolayers shown by SEM images of surface structures after subsection to a tape peel. The inverse monolayer coating withstands tape peel tests, while open-cell reference samples (epoxy micropillars; shown for comparison as insets) are completely damaged. All scale bars are 5mm. Reproduced with permission.<sup>[65]</sup> Copyright 2013, Macmillan Publishers Limited. C) Reflection confocal microscopy images of lubricant-infused surfaces submerged over varying intervals in PBS or air. Reproduced with permission.<sup>[35]</sup> Copyright 2016, Elsevier Ltd.

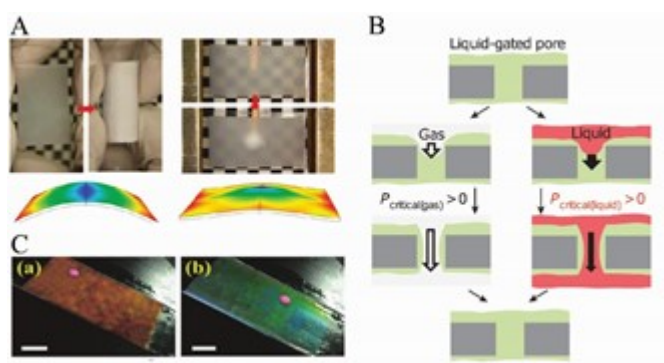


**Figure 7.** Adaptability and responsiveness of liquid-infused materials. A) Above: Images illustrating the change in optical transmission under bending (left) and poking (right). Air pockets induced by mechanical deformations lead to increased light scattering. Below: The corresponding pressure changes predicted by finite-element modelling. Reproduced with permission.<sup>[96]</sup> Copyright 2013, Macmillan Publishers Limited. B) The structural color change of a dynamic slippery inverse opal surface under different stretches. The scale bars are 1.0 cm. Reproduced with permission.<sup>[97]</sup> Copyright 2017, WILEY-VCH Verlag GmbH & Co. C) Hypothesis for gating a pore by liquid reconfiguration. If the pore is filled with a stably held liquid (green), flow of both gases and liquids will be gated by pressure-induced deformation of the gating liquid surface. In the open state, the gating liquid will reversibly reconfigure to form a liquid-lined pore. Each transport substance will have a specific critical pressure based on its ability to overcome the capillary pressure at the liquid-gas or liquid-liquid interface, and the liquid-lined pore will prevent contact with the solid. When the pressure is released, a non-fouled pore returns to its original liquid-filled state. The liquid-based gating mechanism provides a unified strategy for selective, responsive, tunable and antifouling multiphase transport. Reproduced with permission.<sup>[98]</sup> Copyright 2015, Macmillan Publishers Limited.

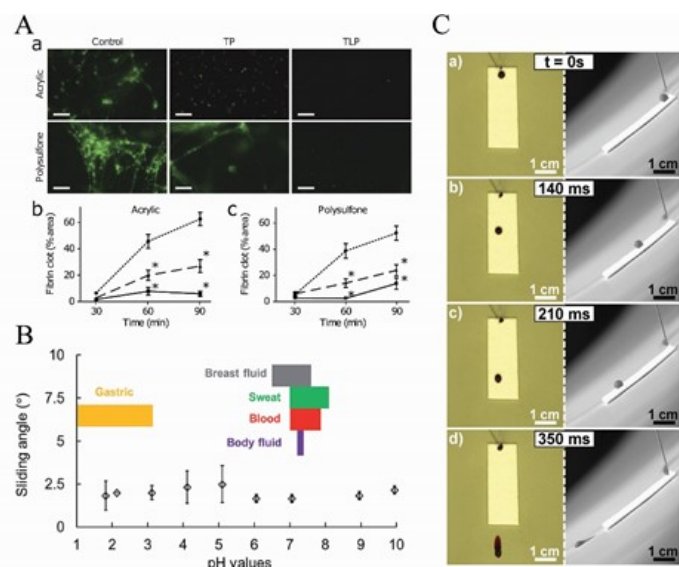


**Figure 8.** Interactions with physiological fluids. A) Whole blood interactions with liquid-infused (TLP) surfaces. a) Fluorescent micrographs of acrylic (upper panels) or polysulfone (lower panels) pieces after 90-min incubation with fresh human blood containing heparin and fluorescent fibrinogen showing polymerized fibrin networks on the control (left column), decreased network formation on hydrophobic (TP, center column) and punctate staining with minimal network formation on TLP (right column). Scale bars, 50  $\mu$ m. b) Graph showing a reduction of percent fibrin-covered area on TLP (full line) acrylic compared to control (dotted line) and TP (dashed line). c) Graph showing a reduction of percent fibrin-covered area on TLP (full line) polysulfone compared to control (dotted line) and TP (dashed line). Reproduced with permission.<sup>[37]</sup> 2014, Nature America, Inc. (B) Time-sequence images of a drop of heparinized human blood rolling down on Gel Blot paper functionalized with C<sub>10</sub><sup>F</sup> (side view: right; front view: left). The tilting angle is 30°. Reproduced with permission.<sup>[49]</sup> 2013, WILEY-VCH Verlag GmbH & Co. (C) shows the sliding angles for various liquids with different pH values. Reproduced under the terms of the Creative Commons CC BY 3.0 license.<sup>[87]</sup> Copyright 2016, The Royal Society of Chemistry.

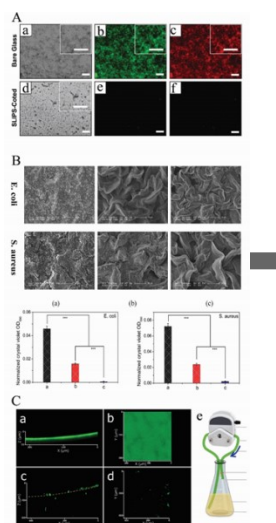


**Figure 9.** Bacterial adhesion. A) Bright-field (a,d) and fluorescence (b,c,e,f) microscopy images of bare glass (a–c) and liquid-infused (d–f) glass substrates after incubation with droplets of *Candida albicans* inocula; droplets were incubated for 3 h, stained, and tilted to permit aqueous fluids to slide away from the original location of the droplet prior to imaging; green fluorescence indicates cytoplasmic staining, red stain marks intravacuolar structures in metabolically active (live) cells. Scale bars, including insets, are 100  $\mu\text{m}$ . Reproduced with permission.<sup>[104]</sup> Copyright 2016, WILEY-VCH Verlag GmbH & Co. B) Above: FESEM images of the surfaces after exposure to *E. coli* and *S. aureus* for 24 h. a) control surface, b) hydrophobic wrinkled surface, and c) liquid-infused wrinkled surface. Scale bar is 20  $\mu\text{m}$ . Below: Crystal violet staining-based quantification of the adherent *E. coli* (left) and *S. aureus* (right) after incubation for 24 h. Reproduced with permission.<sup>[60]</sup> Copyright 2015, American Chemical Society. C) Confocal microscopy of a  $\approx 40$   $\mu\text{m}$  thick *P. aeruginosa* biofilm (green) on untreated (a,b) and infused (c,d) silicone catheter analog after 24 h under flow in setup shown in (e). Adapted under the terms of the ACS AuthorChoice license.<sup>[138]</sup> Copyright 2014, American Chemical Society.

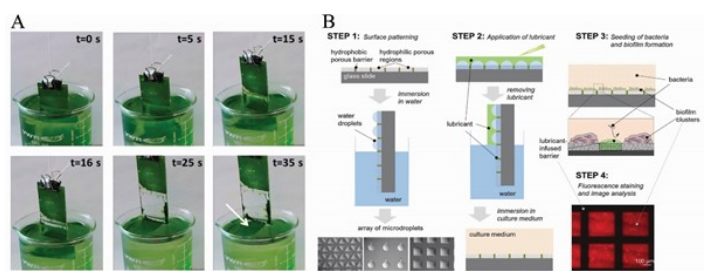


**Figure 10.** Biofilm release from liquid-infused surfaces. A) Glass slides half-coated with lubricant-infused PDMS were incubated in culture vessels containing the green alga *B. braunii*. After 12 days, the slides were slowly removed from the vessel using a dip coater attached to the slide. At  $t = 0$  s and  $t = 5$  s, the clear attachment of the algae biofilm to the untreated glass can be seen. However, at  $t = 15$  s the boundary between the treated and untreated glass is crossed, and at  $t = 16$  s the biofilm begins to peel away from the surface. The white arrow indicates the intact biofilm floating on the surface of the culture medium. Reproduced with permission.<sup>[71]</sup> Copyright 2014, American Chemical Society. B) Formation of patterned liquid-infused surfaces. Step 1: When the hydrophilic–hydrophobic patterned substrate is immersed in water, an array of microdroplets is formed on the hydrophilic areas while the hydrophobic areas remain dry (an effect of discontinuous dewetting). Different geometries of microdroplet arrays are shown. Step 2: A thin layer of Krytox lubricant is applied over the substrate infusing only the nonwetted hydrophobic areas of the porous polymer, forming a liquid-infused surface. The surface is dipped first into water to wash off the excess of Krytox covering the water droplets and then into culture medium to replace water with medium. Step 3: Bacteria cultured on the substrate adhere to the hydrophilic areas but are repelled by the liquid regions. Step 4: Fluorescence staining and image analysis of *P. aeruginosa* biofilm on hydrophilic squares separated by liquid barriers. Reproduced with permission.<sup>[154]</sup> Copyright 2016, WILEY-VCH Verlag GmbH & Co.

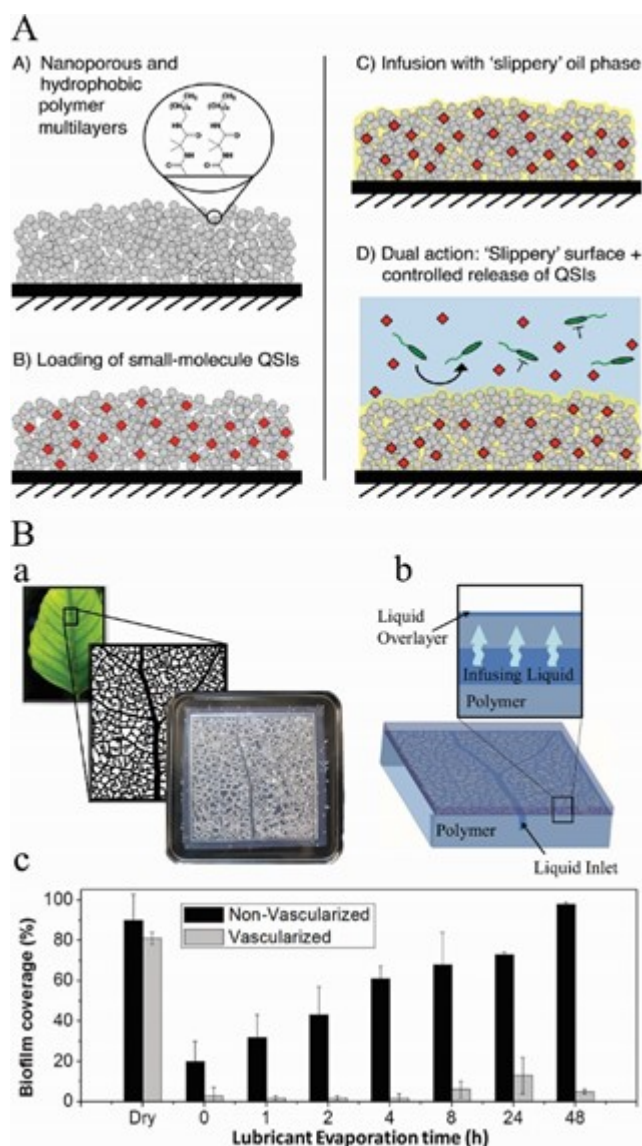


**Figure 11.** Multi-functionality in liquid-infused surfaces for controlling bacterial adhesion. A) Schematic illustration showing the fabrication of quorum sensing inhibitor (QSI)-loaded liquid-infused surfaces. a) Reactive and nanoporous polymer multilayers (gray) are functionalized with n-decylamine to render them hydrophobic. b) Small-molecule QSIs (red) are loaded into the multilayers by adding an acetone solution of the agents to dried films and allowing the solvent to evaporate. c) Silicone oil is infused into the multilayers. d) Loaded liquid-infused surfaces gradually

release QSIs into aqueous solution; the liquid layer prevents the colonization of bacteria directly on the coated surface, and the released QSI modulates the behaviors of nearby planktonic bacteria.

Reproduced with permission.<sup>[105]</sup> Copyright 2016, American Chemical Society. B) A bio-inspired approach to the continuous replenishment of a liquid-infused polymer surface. a) The creation of vascular channels within the polymer matrix, from pattern identification to physical sample creation. The channels can be as complex as the vasculature of a living system such as a leaf, or as simple as a few straight channels. b) Schematic of the mechanism of action. The vascular channels are filled with excess slippery liquid, which diffuses through the polymer to the surface when the overlayer is removed. c) *S. aureus* biofilm coverage for both vascularized and non-vascularized samples after 48 h of evaporation of the liquid overlayer. Reproduced with permission.<sup>[71]</sup> Copyright 2014, American Chemical Society.



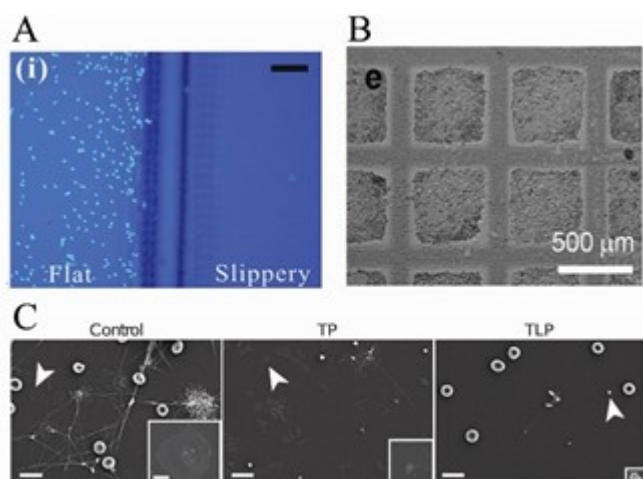


**Figure 12.** Cell interaction. Comparison diagram for C6 glioma cell behavior at the boundaries between flat area and laser-induced roughened, fluoroalkylsilane-modified slippery surface. Scale bar 100 $\mu\text{m}$ . Reproduced with permission.<sup>[36]</sup> Copyright 2018, WILEY-VCH Verlag GmbH & Co. B) HEK 293 cells cultured on a hydrophobic liquid micropattern (500 $\mu\text{m}$  side length square, 100 $\mu\text{m}$  barrier). Reproduced with permission.<sup>[157]</sup> Copyright 2018, WILEY-VCH Verlag GmbH & Co. C) Scanning electron micrographs of acrylic surfaces after 30 min incubation shows reduced platelet adhesion on a liquid-infused surface (TLP) compared to control and hydrophobic (TP) surfaces. Scale bars, 10  $\mu\text{m}$ . Insets show platelet morphology, white arrowheads show platelets. Inset scale bar, 2  $\mu\text{m}$ . Reproduced with permission.<sup>[37]</sup> Copyright 2014, Nature America, Inc.



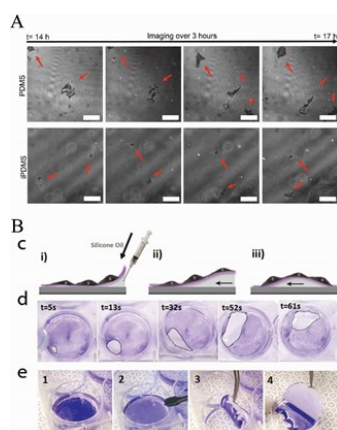


**Figure 13. Cell growth and manipulation.** A) Neonatal dermal fibroblasts imaged 14 h after seeding. The cells on PDMS were attaching and spreading, whereas the cells on infused PDMS (iPDMS) continued to probe the surface and secrete tethers but did not attach. All scale bars are 50  $\mu\text{m}$ . Red arrows indicate the cells that are traversing and exploring the surface. Reproduced with permission.<sup>[88]</sup> Copyright 2017, Steffi Sunny. B) c) Schematic of peeling of the cell sheet off the surface: i–ii) silicone oil is added underneath the mesenchymal stem cells onto the surface of the infused PDMS, in order to allow the oil to penetrate between the surface of the infused PDMS and fibronectin/cellular layer and create a small pool. iii) The pool of silicone oil is moved around the well, delaminating the cell sheet from the surface as it travels. d) Time lapse images of a pool of silicone oil (highlighted by a dotted line) moving around the well and delaminating the sheet from the surface. e) Time-lapse images showing complete, intact cell sheet transfer from the 6-well plate to a petri dish. The cells are stained with crystal violet for easier visualization. 1) The intact cell sheet is first completely delaminated from liquid-infused polymer substrate. 2) A piece of filter paper is placed onto cell sheet. 3) The filter paper with the attached cell sheet is removed from the well. 4) The cell sheet is placed in a petri dish, and the filter paper is removed. Reproduced under the terms of the Creative Commons CC BY license.<sup>[114]</sup> Copyright 2015, Springer Nature.

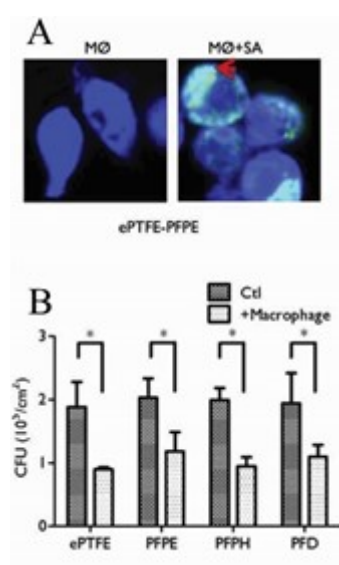


**Figure 14.** Cell functionality. A) Macrophage phagocytosis visualized by confocal microscopy.

CellTrace Violet-labeled macrophages (blue fluorescence) were exposed to Syto-9-labeled *S. aureus* (green fluorescence) for 30 min. MØ: macrophages; SA: *S. aureus*. Red arrow highlights engulfed bacteria. (below). B) The effect of liquid-infused surfaces on the bactericidal potential of macrophages. Macrophages were incubated with *S. aureus* for 2 h and viability was examined by a colony forming unit assay. Reproduced with permission.<sup>[35]</sup> 2016, Elsevier Ltd.

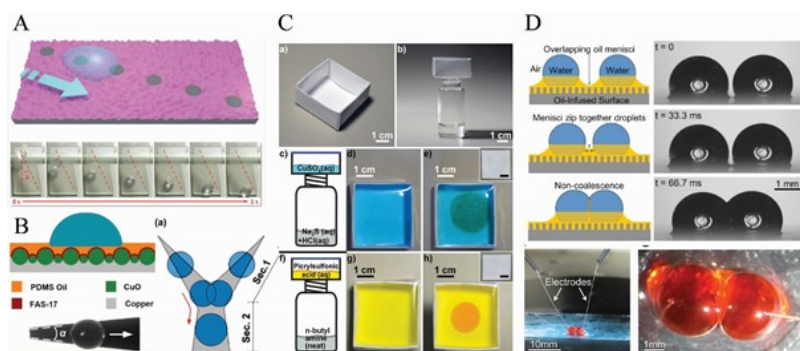


**Figure 15.** Directed droplet movement and compound detection. A) (Above) Graphic representation of the creation of smooth points along a textured surface to create a droplet movement path. (Below) A water droplet sliding along a route on a lubricant-infused film. To preset this movement route, a linear array composed of six flat regions (1 mm diameter, 3 mm apart) was programmed onto a microstructured surface by selectively transferring water droplets onto an untreated film. Reproduced with permission.<sup>[192]</sup> Copyright 2016, American Chemical Society. B) Above left: Schematic diagram of droplet on a liquid-infused CuO surface. Below left: Top view of droplet moving horizontally along the gradient on such a surface. Right: Schematic diagram of droplet aggregation. Reproduced with permission.<sup>[161]</sup> Copyright 2017, American Chemical Society. C) Gas-permeable but liquid-impermeable “chambers” fabricated by folding and creasing  $R^F$  paper and sealing the top with a gas-impermeable tape. This approach can be used to create colorimetric sensors to detect either hydrogen sulfide or volatile primary amines. a) Design of the “chamber” and b) design of the experiment. Each sealed “chamber” contained an aqueous solution of either d)  $\text{CuSO}_4$  or g) picrylsulfonic acid (1 M in water). When the paper structure is exposed to a volatile source of  $\text{H}_2\text{S}$  or butyl amine, the solution in the “chamber” forms e) a brown precipitate ( $\text{CuS}$ ), or h) an orange product (n-butyl-2,4,6-trinitroaniline). The insets depict the bottom of the chamber after the colorimetric detection occurred. Reproduced with permission.<sup>[49]</sup> Copyright 2018, WILEY-VCH

Verlag GmbH & Co. D) (Above) When the oil menisci of two droplets overlapped, an oil film formed between the droplets to enable noncoalescence. (Below) Side-view and top-down photographs of noncoalescing water droplets with inserted electrodes. Reproduced with permission.<sup>[115]</sup> Copyright 2014, the National Academy of Sciences of the United States of America.

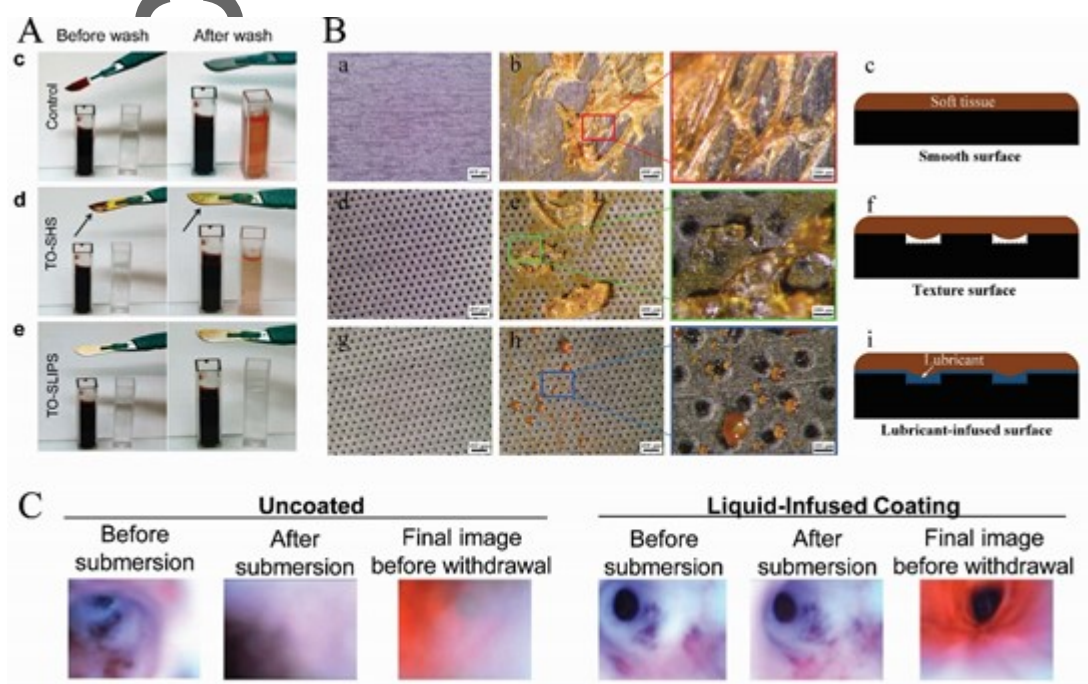


**Figure 16.** Surgical and camera-guided instruments. A) Scalpels were immersed in a cuvette with blood (left column) and blood staining on the scalpel surface was washed off into a cuvette with DI water (right column): c) Untreated, d) Tungsten oxide-superhydrophobic surface (TO-SHS) and e) Tungsten oxide-liquid-infused surface (TO-SLIPS). Untreated and superhydrophobic scalpels were immersed once; the liquid-infused scalpel was immersed three times. Color of the cuvette with DI water indicates and qualitatively correlates with the amount of blood that remains on every sample.

Reproduced under the terms of the Creative Commons Attribution 4.0 International License.<sup>[43]</sup>

Copyright 2015, Macmillan Publishers Ltd. (B) Soft tissue adhesion on the surfaces and the proposed contact models. Panels (a), (d), and (g) are the optical images of smooth stainless steel surface, textured stainless steel surface, and the lubricant-infused surfaces, respectively. Panels (b), (e), and (h) are the optical images after the soft tissue was loaded on the smooth stainless steel surface, textured stainless steel surface, and LIS with stress of 5 N at 250 °C, respectively. Panels (c), (f), and (i) are the proposed contact models for soft tissue on the smooth stainless steel surface, textured stainless steel surface, and LIS, respectively. Reproduced with permission.<sup>[169]</sup> Copyright 2016, Elsevier B.V. C) An endoscope camera image with and without a liquid-infused coating during in vivo bronchoscopy procedures. Reproduced with permission.<sup>[46]</sup> 2016, the National Academy of Sciences of the United States of America.

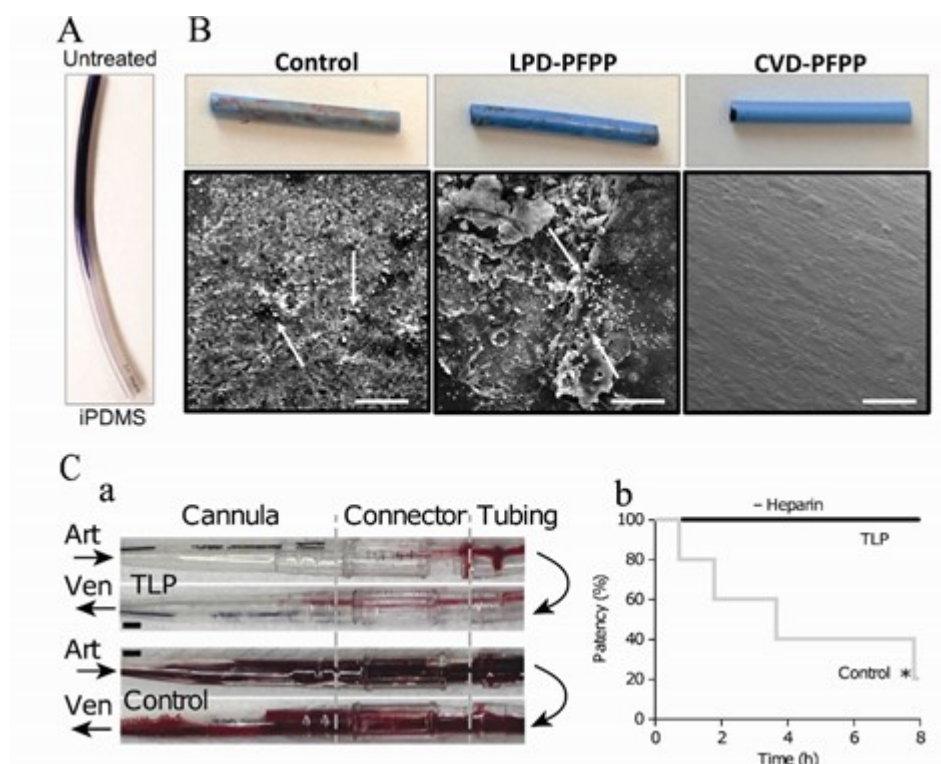


**Figure 17.** Medical tubing with liquid-infused coatings. A) Photograph of crystal-violet-stained biofilms formed on variably infused silicone tubing after exposure to a *P. aeruginosa* culture under flow; the lower half is infused and the top half is untreated. Only a very small amount of biofilms form on the infused section of the tube, and biofilms are clearly present on the untreated section. Adapted under the terms of the ACS AuthorChoice license.<sup>[138]</sup> Copyright 2014, American Chemical Society. B) SEM images of catheters incubated with whole blood. Silanized catheters were stored at room temperature and the blood-catheter interaction was investigated four months after the surface modification procedure. Control, chemical-vapor deposited, liquid-coated (CVD-PFPP) and liquid-phase deposited, liquid-coated (LPD-PFPP) catheters were submerged in whole blood for 15 s prior to imaging. They were subsequently washed with PBS, fixed in 4% formaldehyde for 20 min, and imaged by SEM. Blood clots were formed on control and LPD-PFPP treated catheters

immediately after being in contact with blood. However, no blood clot formation was seen on CVD-PFPP treated catheters. In addition, platelet adhesion (shown with white arrows) was evident on control and LPD-PFPP treated catheters, while no platelets or protein adhesion was seen on CVD-PFPP treated catheters. The scale bars are 50  $\mu\text{m}$ . Reproduced under the terms of the Creative Commons CC BY license.<sup>[70]</sup> Copyright 2017, Macmillan Publishers Ltd. C) a) Photographs of polyurethane cannulae, polycarbonate connectors and PVC tubing of liquid-infused (TLP) (top) and control (bottom) circuits after 8 h of blood flow. Arrows indicate direction of blood flow through arterial (Art) or venous (Ven) cannula. Increased thrombus is visible in the control circuit. Scale bars, 5 mm. b) Kaplan-Meier curve of patency from real-time flow-rate measurements in nonheparinized animals (– heparin) revealed 4 out of 5 control circuits (gray line, n = 5) occlude, whereas TLP circuits (black line, n = 4) remain patent for 8 h. Reproduced with permission.<sup>[37]</sup> Copyright 2014, Nature America, Inc.



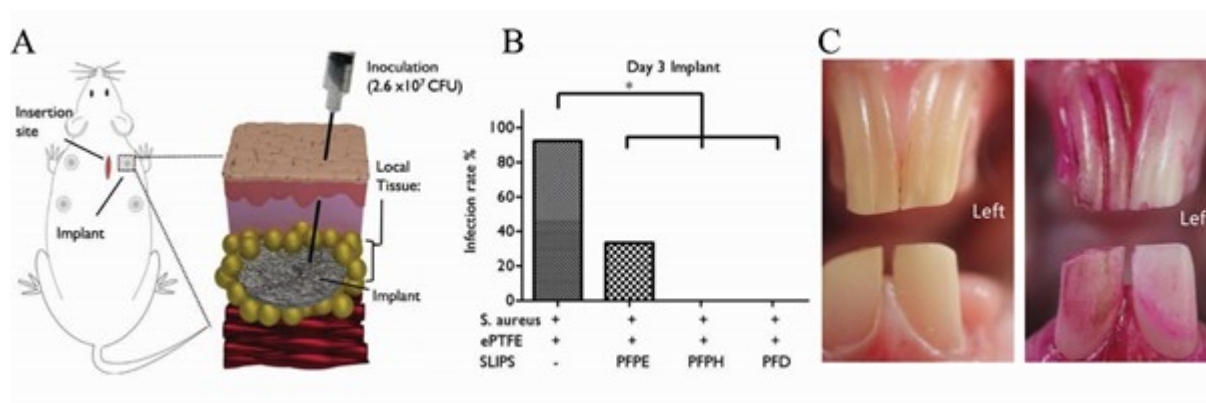


**Figure 18.** Liquid-infused surfaces in vivo. A) Schematic of the in vivo model used to test liquid-infused implants. Circular implants were surgically placed in the subcutaneous tissue on the dorsal side of rat. *S. aureus* was injected 24 h later into the implant site. Three days after bacterial challenge, both the implant and local tissue were harvested. B) Infection rate three days after inoculation. Implants were removed, minced, and sonicated in Luria-Bertani broth and cultured for 20 h at 37°C. Implants were considered infected if broth was turbid (as measured at OD600) and *S. aureus* was present on an agar plate of the culture. Infection rate (%) was calculated by dividing the number of infected implants by the total number of implants (\* $p < 0.05$ ). Reproduced with permission.<sup>[35]</sup> Copyright 2016, Elsevier Ltd. C) Surface appearance of rabbit incisors before (left) and after (right) a 48 h high sucrose diet and 10% fuchsin stain. The left incisors were acid-etched and coated with a liquid layer (SLIPS) while the right incisors were only acid-etched. After the high sucrose diet, less staining was observed on the liquid-infused enamel surfaces than the acid-etched controls. Reproduced under the terms of the Creative Commons CC BY license.<sup>[44]</sup> Copyright 2016, Macmillan Publishers Ltd.



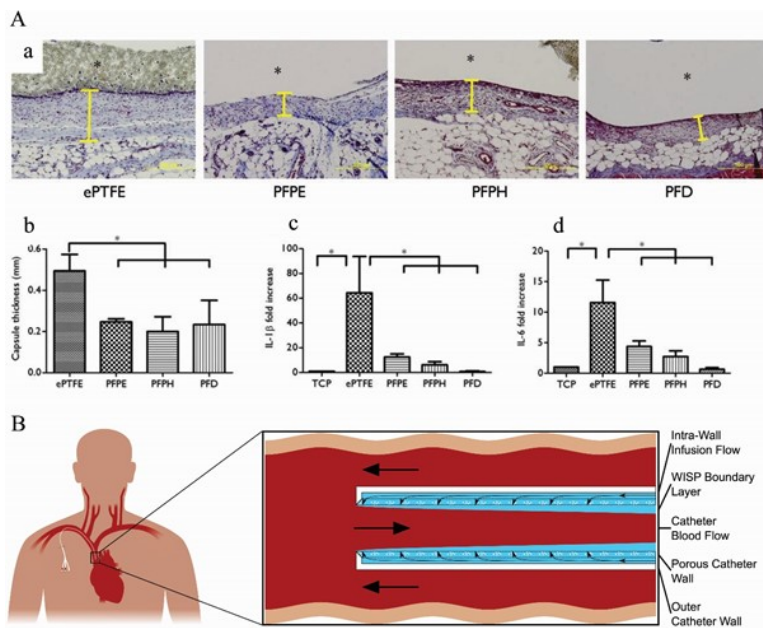


**Figure 19.** Modulating the foreign body response. A) Host response to hernia mesh implants at day 7. Control (ePTFE) or liquid-infused (PFPE, PFPH, PFD) implants were harvested at 7 days. a) Masson's trichrome staining demonstrated a substantially thinner capsule surrounding the liquid-infused implants (Yellow line indicates capsule, \*implant pocket, Scale bar: 500  $\mu$ m). b) Quantification of capsule thickness. c, d) Effect of liquid infusion on macrophage cytokine expression. Macrophages were cultured on tissue culture plastic (TCP), ePTFE or liquid-infused ePTFE (PFPE, PFPH, PFD) for 18 h and IL-1 $\beta$  and IL-6 measured by q-PCR. Error bars represent mean  $\pm$  s.d. from at least 3 replicates, \* $p < 0.05$ . Reproduced with permission.<sup>[35]</sup> Copyright 2016, Elsevier Ltd. B) A water-infused surface protection (WISP) boundary layer prevents thrombotic buildup on the lumen wall of a catheter and provides a means for localized drug delivery. A) Schematic of a proposed central venous catheter in a blood vessel using an intra-wall infusion flow and porous lumen wall in order to create a WISP boundary layer. Reproduced with permission.<sup>[190]</sup> Copyright 2017, International Center for Artificial Organs and Transplantation and Wiley Periodicals, Inc.



**Joanna Aizenberg** is Professor of Materials Science and Chemistry, Director of the Kavli Institute for Bionano Science and Technology, and Platform Leader of the Wyss Institute at Harvard University. She pursues multidisciplinary research that includes bioinspired and smart materials, surface science, and catalysis. She is a member of the American Academy of Arts and Sciences, American Philosophical Society, American Association for Advancement of Science and an External Member of the Max Planck Society.



**Caitlin Howell** is an Assistant Professor of Biomedical Engineering at the University of Maine. She received her Ph.D. from the University of Heidelberg, Germany under the supervision of Professor Michael Grunze, then worked as a postdoc at the Wyss Institute for Biologically Inspired Engineering at Harvard University with Professor Joanna Aizenberg. In 2016, she joined the faculty at the University of Maine where her research focuses on the design and engineering of surfaces and interfaces for the control of biological systems.



**Alison Grinthal** is a Research Scientist in the School of Engineering and Applied Sciences at Harvard University. Her interests span a wide range of fields, including bioinspired engineering, dynamic and adaptive materials, self-assembly, surface and interfacial phenomena, structure and dynamics of macromolecules, and the interplay between chemistry

and mechanics in biological and synthetic systems. She received her B.A. from Swarthmore College in both Chemistry and Anthropology, and received her Ph.D. from Harvard University in Biochemistry.

**Liquid-infused surfaces** provide a new platform for designing biomedical surfaces that not only prevent fouling by physiological fluids, microorganisms, and cells, but also permit the integration of antifouling capabilities with surface functionalities such as dynamic adaptability, drug release, and immune response modulation. These materials can enable new approaches to medical surfaces with applications from diagnostics to surgical equipment and implants.

C. Howell, A. Grinthal, S. Sunny, M. Aizenberg, J. Aizenberg\*

### Designing Liquid-Infused Surfaces for Medical Applications: A review

